To the Graduate Council:

I am submitting herewith a thesis written by Samuel Clark Cropper entitled "Experimental measurements of the capillary pressure - saturation behavior of air and DNAPL in fractured shale saprolite." I have examined the final copy of this thesis for form and content and recommend that it be accepted in partial fulfillment of the requirements for the degree of Master of Science, with a major in Geology.

Larry McKay, Major Professor

We have read this thesis and
recommend its acceptance:

Bill Dunne

Phil Jardine

Accepted for the Council:

Associate Vice Chancellor and
Dean of The Graduate School

EXPERIMENTAL MEASUREMENTS OF CAPILLARY PRESSURE - SATURATION DRAINAGE OF AIR AND DNAPL IN FRACTURED SHALE SAPROLITE

A Thesis
Presented for the
Master of Science
Degree
The University of Tennessee, Knoxville

Samuel Clark Cropper

December 1998

DEDICATION

This thesis is dedicated to my wife

Cheri England Cropper

with love, deep admiration, and deep appreciation.

ACKNOWLEDGMENTS

I would like to offer my thanks and appreciation to all the people who contributed to the completion of this thesis and my education. Dr. Larry McKay supported me and guided my graduate education, while allowing me much-appreciated latitude during my research. Dr. Phil Jardine and Dr. Bill Dunne, members of my thesis committee, and Dr. Steve Driese, temporary committee member, all gave advice which added greatly to the preparation of this manuscript. I would also like to thank Dr. Glenn Wilson for advice in the early stages of my research, and along with Dave Walker, for expert help during the excavation of my sample. Dr. Jacob Dane of Auburn University gave me excellent advice in the later stages of my research.

Other members of the Geology department at the University of Tennessee who helped in various ways during my research include Angie Harton, Dennis Cumbie, Chris Knight, and Dr. Marvin Bennett. I especially thank Melissa Lenczewski for helping me monitor my laboratory setup. Her help was greatly appreciated, especially on weekends, because it allowed me to spend more time at home with my wife Cheri. I would also like to thank Dave King for friendly encouragement when I needed it, and a couch to sleep on when I worked too late to drive home . I would like to thank both Dr. Gary Sayler of the Center for Environmental Biotechnology, and Dr. Don Byerly

of the UT Geology Department for loaning me laboratory space at different stages of my research. Of course, the person to whom I owe the most thanks is my wonderful wife Cheri. Thanks for the time I have taken from you to do this.

Principle financial support for my research was provided by the US Department of Energy Environmental Management Science Program. Additional funding was provided through the UTK Waste Management Resources and Education Institute, the UTK Scholarly Activities Research Incentive Fund, and the UTK Department of Geological Sciences.

ABSTRACT

The drainage behaviors of air-water and DNAPL-water fluid pairs were measured in an 18 cm long column of fractured shale saprolite. Fluorinert™, which is a non-hazardous perfluorocarbon with low solubility and a density of 1.87 g/ml, was used in the experiment as a surrogate for hazardous DNAPLs. The general drainage behaviors of air and Fluorinert were similar. Fracture porosity measurements based on air and Fluorinert drainage were 0.026 and 0.031, respectively. These results are significantly larger than the value of 0.004 estimated from the cubic law, which is calculated from fracture spacing and bulk hydraulic conductivity.

Initial entry of air and Fluorinert into the saprolite column occurred at relatively low capillary pressures, equivalent to 13 and 7.5 cm of water head, respectively. These entry pressures correspond to fracture apertures of 121 and 142 μm respectively, which are significantly larger than the hydraulic aperture of 50 μm predicted from the cubic law. Entry of the non-wetting phase into the matrix porosity occurred at a capillary pressure equivalent to 174 cm of water head for both air and Fluorinert, which correspond to matrix pore throat diameters of 16 and 12 μm, respectively. Predictions of Fluorinert behavior from the air-water data, using a scaling factor based on the fluid interfacial tensions, overestimated the initial fracture entry pressure by 26%, and

underestimated the initial matrix entry pressure by 26%. The disagreement between predicted and measured values is expected to be small relative to the natural variability of fracture aperture and matrix pore size in this material, which suggests that pressure-saturation data from air-water experiments can be used to estimate behavior of other immiscible fluids in this material.

Capillary pressure - saturation relationships were calculated at various elevations within the sample to determine if the capillary pressure calculated at a single constant elevation could be considered representative of a tall sample. It was observed that no single constant elevation represents the capillary pressure of the sample well throughout the drainage. A simple method was proposed to estimate the elevation of the moving immiscible interface within the sample from the applied nonwetting phase pressure and the initial matrix entry pressure. This moving elevation can be used to calculate a capillary pressure that should better represent the pressure conditions throughout the drainage. The van Genuchten (1980) retention relation was fitted to the experimental capillary pressure - saturation curves and provided a better fit than the widely-used Brooks and Corey (1964) model.

TABLE OF CONTENTS

LIST OF TABLES

LIST OF FIGURES

INTRODUCTION

The migration and eventual distribution of dense non-aqueous phase liquids (DNAPLs) in fractured clay-rich materials is distinctly different from DNAPL behavior in unfractured porous materials because of the differences in the distribution of pore or fracture openings in these materials. A DNAPL has sufficiently low water miscibility that it migrates through a porous material as a discrete fluid phase. Entry of the DNAPL into a water-saturated medium occurs when the capillary pressure present at the base of the DNAPL body is equal to or greater than the displacement entry pressure of the largest pore or fracture of the material (Kueper and McWhorter, 1991). The capillary pressure present at the base of a DNAPL body is given by

$$P_c = P_n - P_w \tag{1}$$

where P_c is the capillary pressure, and P_n and P_w are the nonwetting and wetting phase pressures present at the base of the DNAPL body. The displacement entry pressure required for entry into a circular pore is given by (Corey, 1986)

$$P_m = \frac{4\sigma \cos\theta}{2r} \tag{2}$$

where P_m is the displacement entry pressure of the pore, σ is the interfacial tension between the nonwetting (DNAPL) and wetting (water) phases, θ is the contact angle between the DNAPL and the solid medium, and r is the pore radius. The displacement entry pressure required for entry into a fracture is given by (Corey, 1986)

$$P_f = \frac{2\sigma \cos\theta}{2b} \tag{3}$$

where P_f is the displacement entry pressure of the fracture, and $2b$ is the distance between two parallel fracture surfaces. Because the capillary pressure required for entry into fractures is smaller than that required for entry into the much smaller pores of the clay matrix, fractures can act as conduits for DNAPL migration through materials which, if unfractured, would be a capillary barrier for the DNAPL. The resulting DNAPL distribution in the fractured clay is determined by the orientation of the largest connected fractures and could be very erratic. Furthermore, since fractures are typically a small portion of the total porosity of such a material, a DNAPL spill of finite mass, migrating exclusively through fractures, would distribute through a larger volume of material than it would in an unfractured granular material, even if both materials had similar values of total porosity.

Although the entry pressure required for entry into a clay matrix is often higher than would be present in a typical spill situation near ground surface, the capillary

pressure of a DNAPL, and hence its ability to enter small pores, increases with depth. In cases where the continuous body of spilled DNAPL extends to depths of a few meters or tens of meters the initial entry pressure of the clay matrix might be exceeded (Figure 1). In this case, DNAPL would occupy both the fractures and some portion of the matrix porosity. When the DNAPL begins to migrate from the fractures into the matrix porosity, less of it is available to distribute through the fracture system, and the DNAPL is confined to a smaller volume of material. Since most of the total porosity of the material is in the matrix, the total volume of contaminated material is potentially much less. In a modeling study of DNAPL migration in a fractured porous rock, Slough et al., (in review) showed that exceeding the matrix entry pressure can have a significant influence on the overall extent of DNAPL migration. These issues are significant to estimation of the volumes of material contaminated by a DNAPL as well as the choice of a remediation strategy because it may require a very different strategy to remediate or mobilize DNAPL in matrix pores than it would if the DNAPL was exclusively in fractures.

Because DNAPL migration and distribution are largely controlled by capillary behavior, any attempt to estimate or model its movement in a material requires determination of the capillary pressure behavior of the DNAPL in that material. Saturation is a function of capillary pressure in a sample. Procedures to measure capillary behavior versus saturation, (hereafter referred to as the P_c-S relation) were

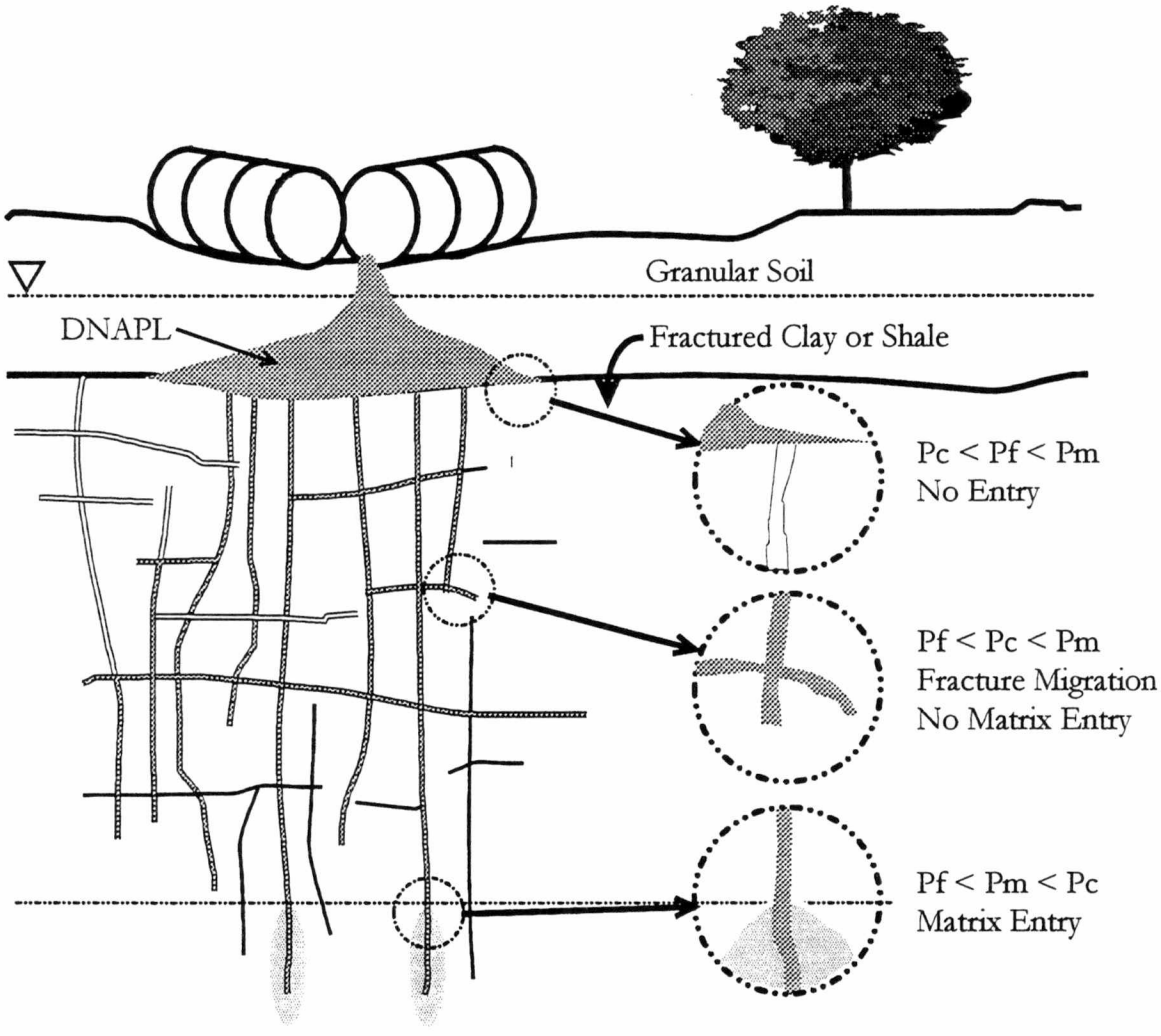

Figure 1. Conceptualization of DNAPL distribution in fractured clay-rich materials.

first developed to study air-water relations for agriculture, and hydrocarbon-water relations for petroleum production. More recently, the same concepts and procedures were successfully applied to immiscible contaminants such as DNAPLs in groundwater (Lin et al., 1982; Kueper et al., 1989). Thus the capillary behavior of a DNAPL in an unfractured material such as the clay matrix is easily determined using standardized procedures, and can be represented by retention functions such as those of Brooks and Corey (1964) or van Genuchten (1980). The Brooks and Corey retention function is given by (Brooks and Corey, 1964)

$$S_e = \frac{S - S_r}{1 - S_r} = \left(\frac{P_d}{P_c}\right)^{\lambda} \quad \text{for } P_c > P_d \tag{4}$$

$$S_e = 1 \quad \text{for } P_c \le P_d \tag{5}$$

where S_e is the effective wetting-phase saturation, S is the wetting-phase saturation, S_r is the residual wetting-phase saturation, P_d is the displacement entry pressure, P_c is the capillary pressure, and λ is a pore-size distribution index. The van Genuchten retention function is given by (van Genuchten, 1980)

$$S_e = \frac{S - S_r}{S_s - S_r} = \frac{1}{[1 + (\alpha P_c)^n]^m} \quad \text{for} \quad P_c > P_d \tag{6}$$

$$S_e = 1 \quad \text{for } P_c \le P_d \tag{7}$$

where S_s is the wetting-phase saturation at a capillary pressure equal to zero, and α, n, and m are fitting parameters. These retention functions can then be incorporated into computer models designed to estimate DNAPL migration in the material.

If the entry pressure at which an immiscible phase enters a material is known, then the fracture or pore size it first entered can be estimated using equation 2 or 3. It follows that the entry pressure at which another immiscible phase would enter the same material can be predicted from

$$P_{d2} = \frac{\sigma_2 \cos\theta_2 P_{d1}}{\sigma_1 \cos\theta_1} \tag{8}$$

where P_{d2} is the predicted entry pressure of the second fluid, P_{d1} is the entry pressure of the measured fluid, σ_1 and σ_2 are the interfacial tensions of the two fluids, and θ_1 and θ_2 are the contact angles between each fluid and the soil minerals. Experimental studies by Dumore and Scholls (1974) and Lenhard and Parker (1987) demonstrated that the P_c-S behavior of one immiscible fluid can be scaled by the ratio of interfacial tensions to give a good approximation of the P_c-S behavior of other immiscible fluids in the same material. This implies that the contact angle does not change significantly and that for equivalent saturations, the capillary pressure relationship between two different immiscible fluids in the same material can be approximated by

$$P_{c2} = \frac{\sigma_2 P_{c1}}{\sigma_1} \tag{9}$$

If this approximation is also applicable in fractured materials, the capillary behaviors of hazardous DNAPLs such as trichloroethene or perchloroethene could be predicted from the measured capillary behavior of a non-hazardous immiscible fluid such as air.

When fractures are present and the matrix porosity of a material has a high entry pressure, DNAPL migration will occur exclusively in the fractures, so the capillary behavior of the fracture system is of interest. In such a material, the P_c-S behavior should be measured directly in the fractures. Reitsma and Kueper (1994) measured the capillary behavior of a single horizontal fracture in a laboratory sample of massive dolomitic limestone. They found that traditional P_c-S measurement procedures worked well in this situation. The single fracture exhibited the expected capillary behavior and the observed P_c-S relationship was easily fit by the Brooks and Corey model. In this approach, the Brooks and Corey pore-size distribution index, λ, is replaced by an aperture-size distribution index.

Although the Brooks and Corey approach proved adequate for the single-fracture case investigated by Reitsma and Kueper (1994), traditional procedures for measuring capillary behavior may not be directly applicable to systems of fractures. The standard procedure for measuring capillary behavior consists of applying a nonwetting fluid at a known pressure to a sample of the material to be analyzed, waiting for an equilibrium

condition, and then determining the saturation of wetting phase in the sample (Klute, 1986). This procedure produces one pressure-saturation data pair. Additional data pairs are produced by incrementing the nonwetting fluid pressure. These data produce an equilibrium pressure-saturation drainage curve that can then be fit to the Brooks and Corey retention function, or one of several other such empirical relationships (van Genuchten, 1980; Su and Brooks, 1975) to describe the capillary behavior of the sample. This approach assumes that one data pair of pressure and saturation values can represent the entire sample at each equilibrium condition.

However, when the densities of the nonwetting and wetting fluids are different, the capillary pressure, P_c varies with height within the pressure cell according to the equation (Liu and Dane, 1995)

$$P_c(z) = P_n(z) - P_w(z) \tag{10}$$

where z is the elevation of the interface between fluids within the pressure cell, $P_n(z)$ is the non-wetting fluid pressure at z, and $P_w(z)$ is the wetting fluid pressure at z. General expressions derived by Liu and Dane (1995) to determine $P_n(z)$ and $P_w(z)$ for various pressure cell configurations were adapted for use with the pressure cell configuration used in this study (Figure 2). They are given by

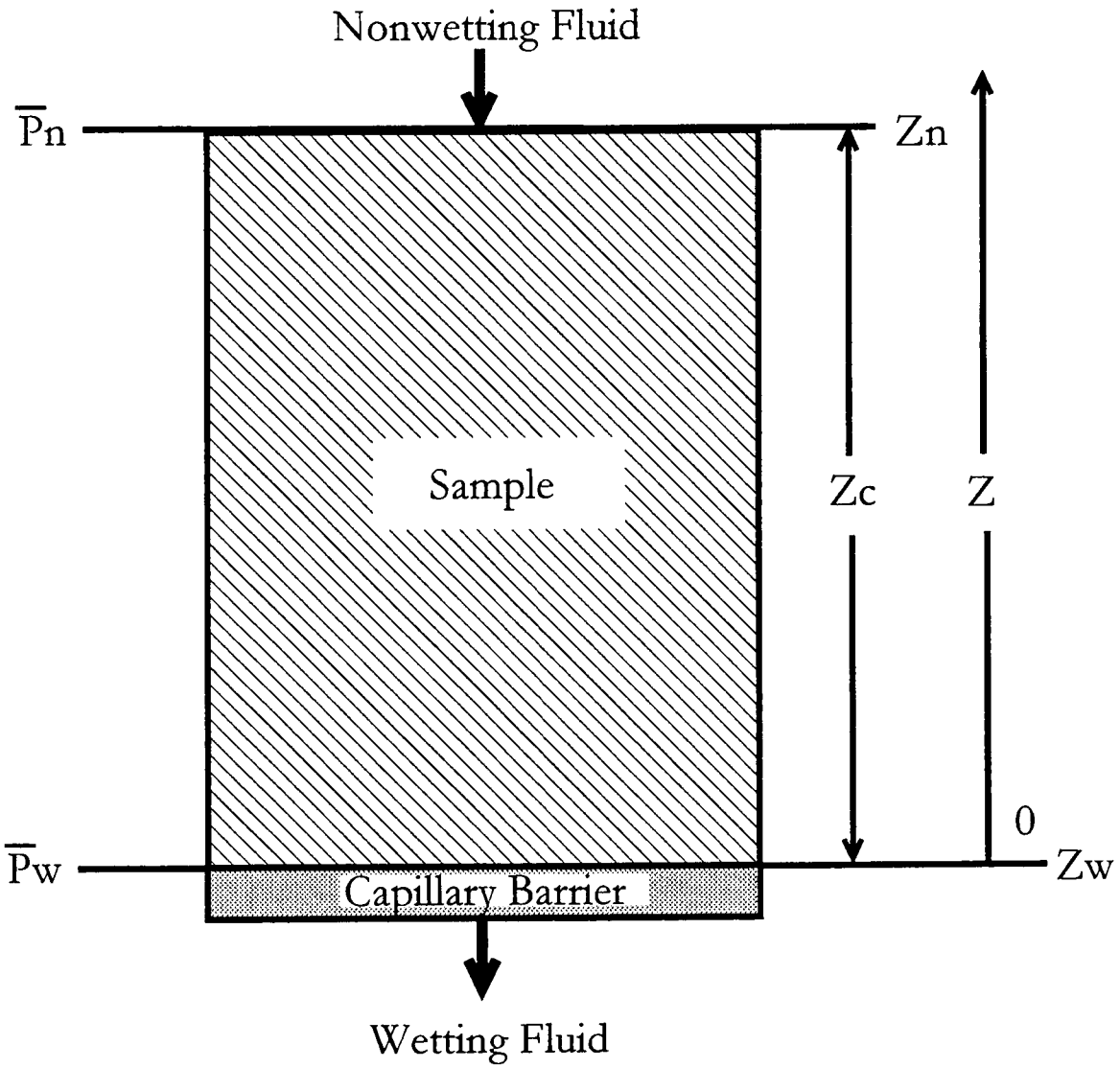

Figure 2. General pressure-cell configuration. The nonwetting phase pressure ($\overline{P}n$) is measured at the sample influent level (Zn), and the wetting-phase pressure ($\overline{P}w$) is measured at the sample effluent level (Zw). The elevation datum is the sample effluent level (Zw).

$$P_n(z) = \overline{P_n} - \rho_n g(z - z_n) \tag{11}$$

for $\rho_n < \rho_w$

$$P_w(z) = \overline{P_w} - \rho_w g(z - z_w) \tag{12}$$

and

$$P_n(z) = \overline{P_n} - \rho_n g(z_n - z) \tag{13}$$

for $\rho_n > \rho_w$

$$P_w(z) = \overline{P_w} - \rho_w g(z_w - z) \tag{14}$$

where $\overline{P_n}$ and $\overline{P_w}$ are the nonwetting- and wetting-fluid pressures measured at z_n and z_w (Figure 2), ρ_n and ρ_w are the nonwetting- and wetting-fluid densities, and g is the gravitational field strength. Because pressure varies with height within the sample, one pressure value cannot represent the pressure conditions everywhere within a tall sample, but is only representative of one elevation within the sample. Because of this limitation, the standard procedure for measuring capillary behavior suggests that samples should be less than 2 cm tall (Klute, 1986). The variation of capillary pressure with height in a sample of this height is negligible in comparison to the relatively large capillary pressures needed to drain the wetting fluid from small pores to residual content. Thus, little error is introduced by assuming that capillary pressure measured at one elevation within the sample is representative of values throughout the sample. This height constraint presents a problem for fractured samples. Large undisturbed

columns or pedons are often needed to obtain a representative sample of the heterogeneity in a fractured system. In these cases, capillary pressure variations with height may be significant in relation to the lower capillary pressures at which fractures would drain, and hence, the height of the sample cannot be neglected.

If pressure variations with sample height are not neglected, equilibrium saturations may not be representative of the entire sample either. If a sample is short and it is assumed that one pressure measurement represents values throughout the sample, the volume of wetting fluid displaced at a given equilibrium condition is usually assumed to have drained from equal-sized pores throughout the sample. In a homogeneous material, these pores would be uniformly distributed through the sample, thus the displaced fluid would come equally from all parts of the sample, and the saturation value at any equilibrium step would apply to the whole volume of material. If a fractured sample is tall, the elevation of the interface between immiscible phases within each fracture would be a function of the fracture aperture and pressure conditions at each equilibrium step. Thus, it may not be assumed that the wetting fluid was displaced uniformly from the whole volume of the sample because of the distribution of capillary pressures from top to bottom of the sample. For these reasons the P_c-S relation of a tall column cannot be considered as an aperture-size distribution relation. These issues substantially increase the difficulty in determining a representative

relationship for the capillary pressure versus saturation relationship in fractured materials.

The primary objectives of this study are: 1) to experimentally determine the capillary drainage behavior of two immiscible fluids in the same tall sample of fractured clay-rich material and to determine initial entry pressure of the fractures, initial entry pressure of the matrix, and the general drainage behavior of the fracture systems; 2) to evaluate the possibility of predicting initial fracture entry and initial matrix entry of a DNAPL from air-water measurements in this material; and 3) to explore the applicability of using the Brooks and Corey or van Genuchten retention relationship to describe the drainage behavior of a tall fractured sample.

MATERIALS AND METHODS

Field Site and Previous Investigations

The material used for capillary drainage measurement in this study is fractured shale saprolite excavated from a research site in Solid Waste Storage Area 7 (SWSA 7) on the Oak Ridge Reservation (ORR) in eastern Tennessee (Figure 3). The site is underlain by the upper unit of the Dismal Gap Formation of the Conasauga Group, which is Middle Cambrian in age (Rothschild et al., 1984; Hatcher et al., 1992). The saprolite, or isovolumetrically weathered and decomposed bedrock, is soft enough that it can be excavated by hand tools, but retains the bedding features and fractures of the underlying unweathered limey shale to limestone parent rock. Petrographic research indicates that there are two distinct saprolite types at the site, (Penfield, 1998) representing two parent lithologies. Calcareous siltstone beds weathered to a silty, thin-bedded saprolite, and limestone beds weathered to a weakly consolidated, more thickly bedded saprolite. The saprolite has three distinct fracture sets (Dreier et al., 1987). One set consists of bedding-plane-parallel fractures and the other two sets are joint sets that are perpendicular to the bedding planes and perpendicular to each other. The bed parallel fractures were clay-filled or clay-lined and the bed-normal sets were often of larger aperture (Penfield, 1998). The silty saprolite also has numerous, much smaller fractures which were not observed in the limestone saprolite.

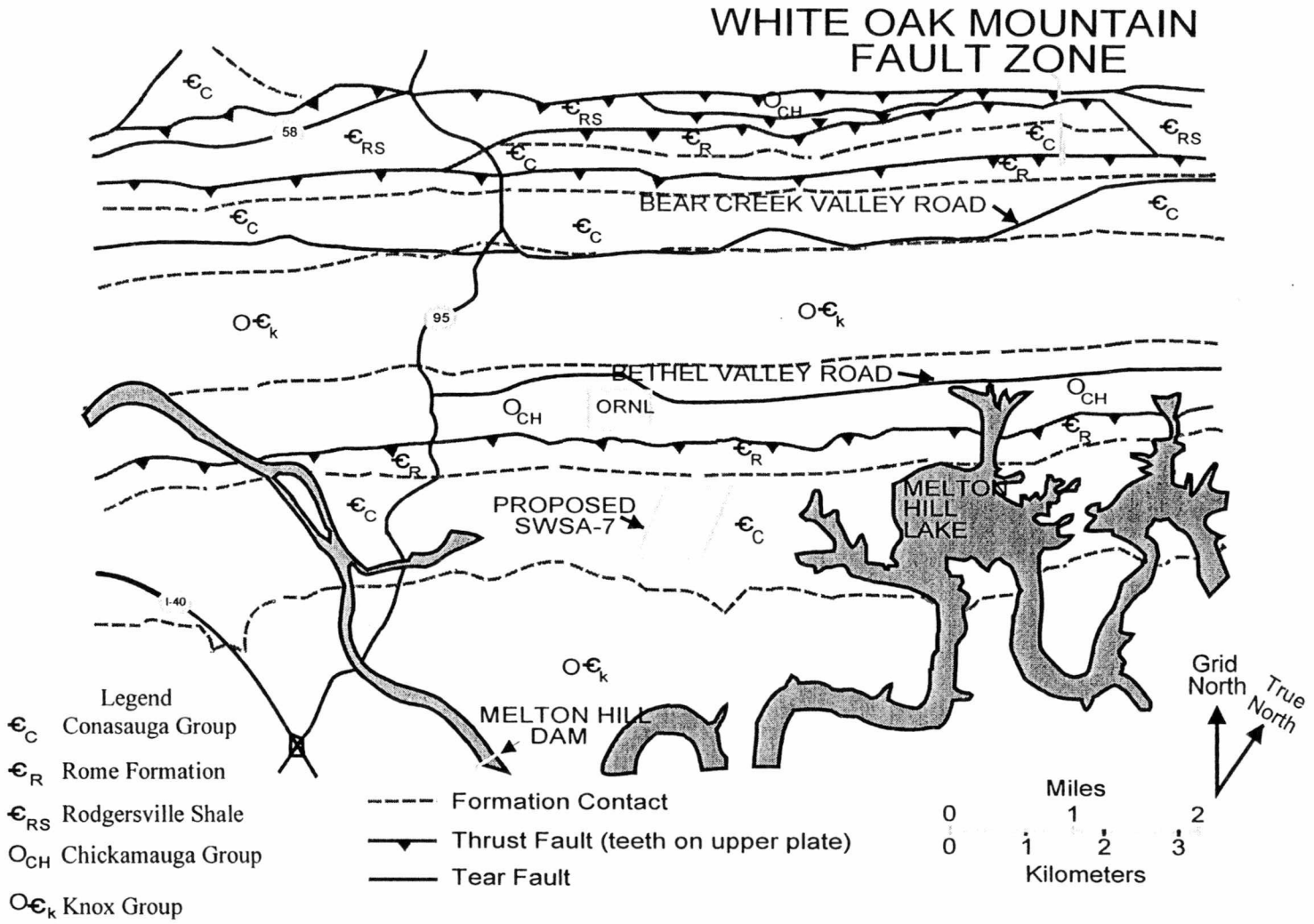

Figure 3. Location map of proposed SWSA-7 site. (adapted from Rothchild et al., 1984).

The saprolite at the study area was the subject of many previous investigations of subsurface hydrology and contaminant transport. Field and laboratory experiments (Jardine et al., 1988; Wilson et al., 1993; Reedy et al., 1996) showed that solute transport is influenced by advection through the fractures combined with diffusion into the relatively immobile porewater in the fine-grained matrix. Laboratory experiments (Harton, 1996; Cumbie, 1997; Haun et al., 1998) in undisturbed columns showed that colloids are largely excluded from the matrix, and hence are transported much more rapidly than solutes.

The previous studies at the site demonstrated considerable heterogeneity in the saprolite. Cumbie (1997) carried out tracer experiments on an undisturbed column of the saprolite collected from a depth of 1 to 1.5 meters and then disassembled it to study fracture spacing. He reported mean spacing of 0.9 cm for the bedding plane fractures and 2.7 cm for the joints, but the distribution of tracers on fracture surfaces indicated that not all fractures were hydraulically active. The spacing of "active" fractures was approximately 2.5 cm for both the bedding plane and orthogonal sets. Other researcher have reported fracture spacing ranging from .005 to .04 meters (Dreier et al., 1987; O'Brien et al., 1996; Harton, 1996). Saturated bulk hydraulic conductivity values reported from both field and laboratory measurements in the upper two meters of saprolite range from 7.6 x 10-6 m/s to 1.4 x 10-4 m/s (Wilson et al., 1989; Harton, 1996). In field measurements of hydraulic conductivity at different degrees of

saturation, Wilson et al. (1992) observed that fractures drained as saturation decreased from 1 to 0.91, and hydraulic conductivity values decreased three orders of magnitude. They predicted saturated hydraulic conductivity of the matrix to be between 4.3×10^{-8} m/s and 6.5×10^{-9} m/s. Hydraulic aperture values calculated from the cubic law (Snow, 1968), and measured values of hydraulic conductivity and fracture spacing for large undisturbed samples of saprolite from the study site, ranged from 30 μm to 102 μm (Harton, 1996; Haun et al., 1998;Cumbie, 1997). A summary of reported values of pertinent physical properties is shown in Table 1. These values were all determined in large undisturbed samples of the saprolite from the field site, and show a high degree of heterogeneity even though each of the samples was excavated from a depth between 1 and 1.5 meters and within 3-4 meters of each other.

The capillary behavior of small undisturbed samples of the saprolite was measured by Wilson et al. (1992). The behavior indicated drainage of the macroporosity to residual saturation at capillary pressures between 0 and 1.0 kPa. Drainage from the matrix porosity began at 29.5 kPa and continued to the end of the study at 980 kPa. The capillary behavior of small samples of the clay matrix between fractures was measured by the mercury porisimetry method (Dorsch and Katsube, 1998). This study measured the drainage behavior between 140 kPa and 420 MPa, which characterizes the porosity of pore throats smaller than 10 μm. The pore-size distributions were highly variable from sample to sample and indicate a high degree of heterogeneity in

Table 1. Summary of saprolite properties measured in undisturbed columns excavated from the study site.

Study	Saturated Hydraulic Conductivity (m/s)	Porosity (m^3/m^3)	Fracture Spacing (m)	Hydraulic Aperture (μm)
Jardine et al., 1993	4.0×10^{-5}	0.42 - 0.55	-	-
O'Brien et al., 1996	1.7×10^{-5}	-	0.015 - 0.04	-
Harton, 1996	1.4×10^{-4} to 9.1×10^{-5}	-	0.01	102
Cumbie, 1997	2.2×10^{-5}	0.42	0.005 - 0.03	69
Haun et al., 1998	2.9×10^{-6}	0.49	Assumed 0.025	30
Current Study	4.0×10^{-6}	0.54	Assumed 0.025	50

pore sizes within the matrix porosity due to lithologic heterogeneity and degree of chemical weathering. The geometric mean of the matrix pore radius ranged between 0.01 μm and 0.04 μm for less weathered samples, and between 0.14 μm and 1.170 μm for more weathered samples. For the less weathered samples, few pores had a radius larger than .01 μm , while for the more weathered samples there was significant porosity in pores between 0.01 μm and 10 μm. In general, less than 3% of the matrix porosity of all samples was in pores with a radius larger than 5 μm.

Sample Excavation and Setup

Excavation of the undisturbed sample for the current study used procedures developed by previous researchers to minimize fracture disturbance (Jardine et al., 1993; Cumbie, 1997). The cylindrical sample was excavated so that its long axis was oriented parallel to the bedding, which dips at 69 degrees to the southeast. The long axis of the sample is thus parallel to both the bedding plane fracture set and one of the extension sets, which are roughly perpendicular to each other. Bedding strike is N34E. The sample was excavated from a depth of 90 to 108cm below ground surface. Its final dimensions were 18cm long, and 10 cm diameter.

The saprolite sample was placed within a PVC casing and epoxy was pored into the annulus to prevent fluid flow between the sample and the casing. A porous ceramic

plate with an air entry pressure of 50 kPa was placed in direct contact with the effluent end of the sample and firmly attached with more epoxy. End caps with influent and effluent connections were then attached to each end of the column. The completed pressure cell did not leak when tested at water pressures of up to 29 kPa.

Hydraulic Conductivity Testing

The sample was saturated with degassed 0.005 M $CaCl_2$ over a period of several days to maximize saturation of the sample. This fluid was used as the saturation fluid throughout the study. It was chosen to avoid dispersion of the clay in the sample. The saturation fluid was applied to the bottom of the column by raising the applied head in 1 to 2 cm increments to minimize air trapped in the fracture system. The hydraulic conductivity of the sample was then determined using a constant head permeameter, both before and after installation of the capillary barrier. The hydraulic aperture was determined from the measured hydraulic conductivity and fracture spacing using the cubic law (Snow, 1968; 1969)

$$2b = \left[\frac{(K_z - K_m) * 2B * 12 * \mu}{\rho * g} \right]^{(1/3)} \tag{15}$$

where $2b$ is the hydraulic aperture, K_z and K_m are the hydraulic conductivity of the bulk material and of the matrix respectively, $2B$ is the fracture spacing, μ is the dynamic viscosity of water, ρ is the density of water, and g is the acceleration due to gravity.

Immiscible Fluids

In the first set of P_c-S measurements, air was used as the immiscible fluid measured in the sample. The sample was then slowly re-saturated with degassed 0.005 M $CaCl_2$ to bring the sample back to near complete saturation. The second immiscible fluid used was Fluorinert™ FC-40, a multi-purpose non-hazardous perfluorocarbon manufactured by 3M Corporation. Perfluorocarbons were found suitable for use as surrogate DNAPL contaminants by Miller (pers. comm.) because of their physical similarity to common DNAPL contaminants such as perchloroethene. The physical properties of Fluorinert™ FC-40 as reported by the 3M product manual (1995) are: density = 1.87 g/ml; water solubility = 7 ppm; and viscosity = 2.2 centistokes. Miller (pers. comm.) reported an interfacial tension of 52 dynes/cm (5.2×10^{-2} N/m).

Capillary Pressure-Saturation Measurements

The air and Fluorinert measurement setups are shown in Figure 4. The drainage behavior of the sample was determined by injecting the nonwetting fluid at the influent end of the column, with pressure controlled by a digital screw pump designed by GDS Instruments Ltd. for this purpose. The pressure controller could maintain injection pressure targets set by the operator in the operating range of 0 to 100 kPa. The control transducer could resolve pressure changes to 0.01 kPa and pressure targets could be in increments as small as 0.025 kPa. Incrementing the applied pressure raised the nonwetting fluid pressure in the cell because the nonwetting fluid could not pass out of the column through the ceramic capillary barrier. This increase in nonwetting pressure created a temporary total pressure gradient in the column. In response to this imposed gradient, the wetting fluid passed through the capillary barrier and through the effluent tubing into a collection flask until equilibrium was regained. In this way, the nonwetting fluid pressure was incremented while the wetting fluid pressure stayed constant, controlled by the elevation where the effluent tubing was open to the atmosphere. Data collected during drainage are in the form of a nonwetting pressure at the influent end of the sample (at z_n), the volume of water displaced from the sample through the effluent line, and the volume of nonwetting phase injected by the pressure controller. Pressure in the wetting phase is constant and was controlled by the elevation of the outlet of the effluent line. The time allowed for equilibrium to be

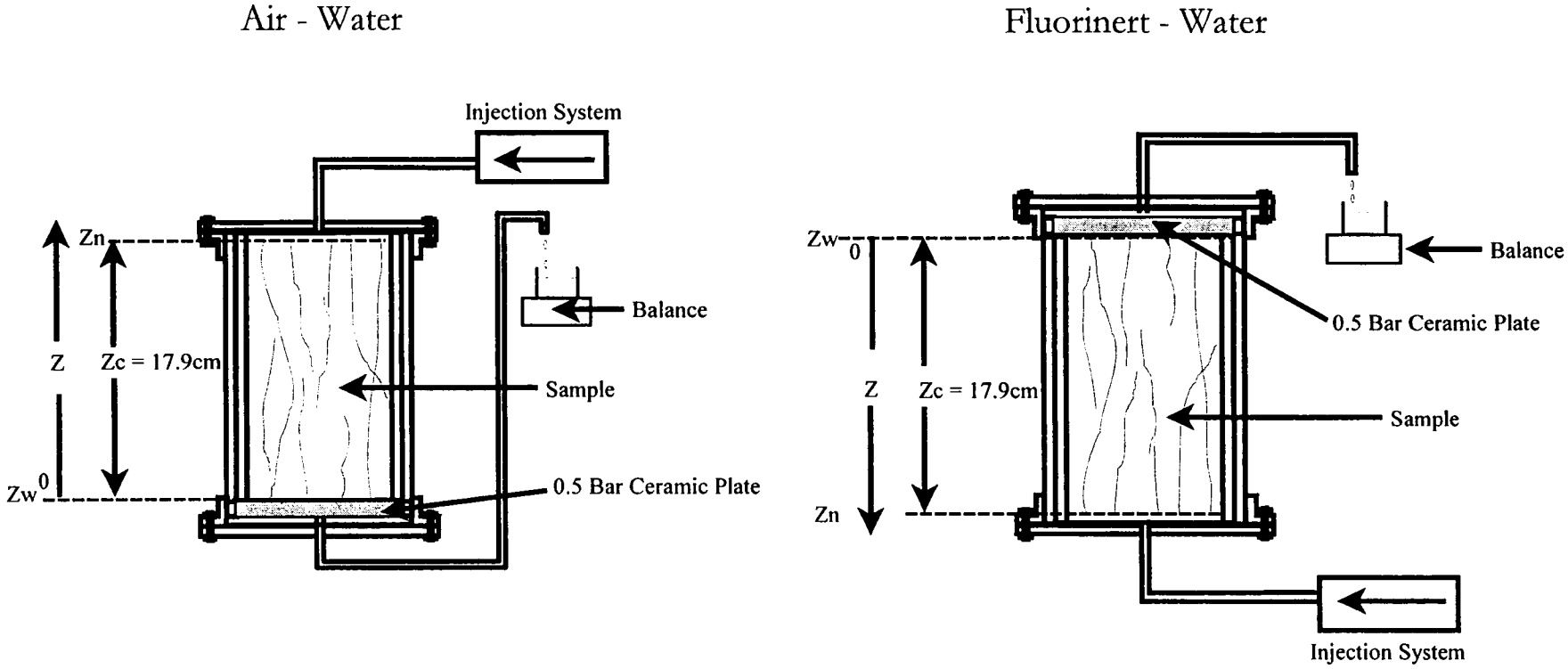

Figure 4. Laboratory setups for air-water and Fluorinert-water injections.

established for each pressure increment was judged by the operator from continuously displayed information on volume and pressure change reported by the data logging equipment. During both injections, target pressure increments gradually increased from .025 kPa at the beginning of the injection to 1kPa as the total applied pressure reached the upper limit.

Because air is less dense than water, it was injected from the top. The sample was oriented so that the flow direction corresponded to the in-situ groundwater flow direction. The effluent tubing was open to the atmosphere at an elevation of 19 cm above the soil effluent level so that a 1.1 cm column of water was above the soil influent level at the start of pressure increments. The elevation of the visible air/water interface in the influent tubing was monitored for the first few pressure targets before the interface moved into the pressure cell and was no longer visible. When several pressure increments failed to displace additional water from the sample, the air was interpreted to be in contact with the soil at the influent end of the column, but at capillary pressures lower than the initial fracture entry pressure. Fluid displaced from this point onward was considered to be from the sample. Because the elevation at which the effluent tubing was open to the atmosphere was constant, the wetting fluid pressure, $\overline{P_w}$ at z_w was also constant at 1.86 kPa throughout drainage. During the air injection, 84 pressure targets were set over the pressure range of 0 to 22.0 kPa. The

average target increment was 0.20 kPa. Equilibrium times varied from a few minutes up to 21 hours. The air injection lasted 13 days.

Fluorinert was injected from the bottom because it is denser than water. The pressure cell was inverted so that the flow direction was the same as during the air injection. The controller reservoir was filled with Fluorinert and pressure increments began with a Fluorinert/water interface visible in the influent line. As before, the elevation of this interface was monitored until it entered the pressure cell during the first few pressure targets. When several pressure increments failed to displace additional water from the sample, Fluorinert was interpreted to be in contact with the influent soil level, but at capillary pressures lower than the initial fracture entry pressure. Water displaced from this point onwards was considered to be from the sample. The effluent tubing was open to the atmosphere at 18.25 cm above the saprolite influent level z_n so the wetting phase pressure $\overline{P_w}$ at z_w was constant at 1.79 kPa throughout the injection. Pressure increments continued until a rapid drop in nonwetting phase pressure and the inability of the pressure controller to attain pressure targets indicated a leak through or around the ceramic plate at 25.2 kPa. A total of 153 pressure targets were set during the Fluorinert injection. The average target increment was 0.14 kPa. Equilibrium times varied from a few minutes up to 184 hours. The Fluorinert injection lasted 54 days.

RESULTS AND DISCUSSION

Hydraulic Conductivity and Aperture

Saturated hydraulic conductivity values for the column measured before installation of the capillary barrier ranged from 2.9×10^{-6} to 4.6×10^{-6} m/s with a mean of 4.0×10^{-6} m/s. The "hydraulic aperture" value for the column was 50 μm. This value was calculated using the cubic law (equation 15), with a bulk hydraulic conductivity of 4.0×10^{-6} m/s, an "active" fracture spacing of 2.5 cm based on Cumbie, (1997), and a matrix hydraulic conductivity of 4.0×10^{-8} m/s. This matrix hydraulic conductivity was based on the predictions of Wilson et. al. (1992). The fracture porosity determined from the hydraulic aperture and the measured fracture spacing was 4×10^{-3}, which was much smaller than the measured bulk porosity of 0.54. Estimated volume of fractures based on the sample dimensions and the cubic law derived value of fracture porosity is 7 cm^3. After the capillary barrier was installed, hydraulic conductivity was again measured yielding a value of 1.1×10^{-6} m/s. This value was deemed sufficient to allow for rapid water drainage during the air and Fluorinert injections.

Capillary Pressure Measurements

The results of the air injection are plotted as the capillary pressure calculated at the sample influent level as a function of the volume of water displaced from the sample (Figure 5). The results of the Fluorinert injection are plotted as the capillary pressure calculated at the sample influent level as a function of the volume of Fluorinert injected into the sample (Figure 6). The volume of Fluorinert injected was used in place of the volume of water displaced because a power interruption during the Fluorinert injection caused a partial loss of data for the volume of water displaced. Because Fluorinert is virtually incompressible and insoluble in water, the volume of Fluorinert injected should very closely approximate the volume of water that was displaced.

Initial Fracture Entry

The initial entry of air into the saprolite macroporosity occurred at a capillary pressure of 1.28 kPa and the initial entry of Fluorinert occurred at 0.73 kPa. These pressures were identified as the first significant displacement of fluid from the sample following several pressure increments with little or no water displaced. Assuming that the geometry of the fractures in the sample can be represented as two parallel plates,

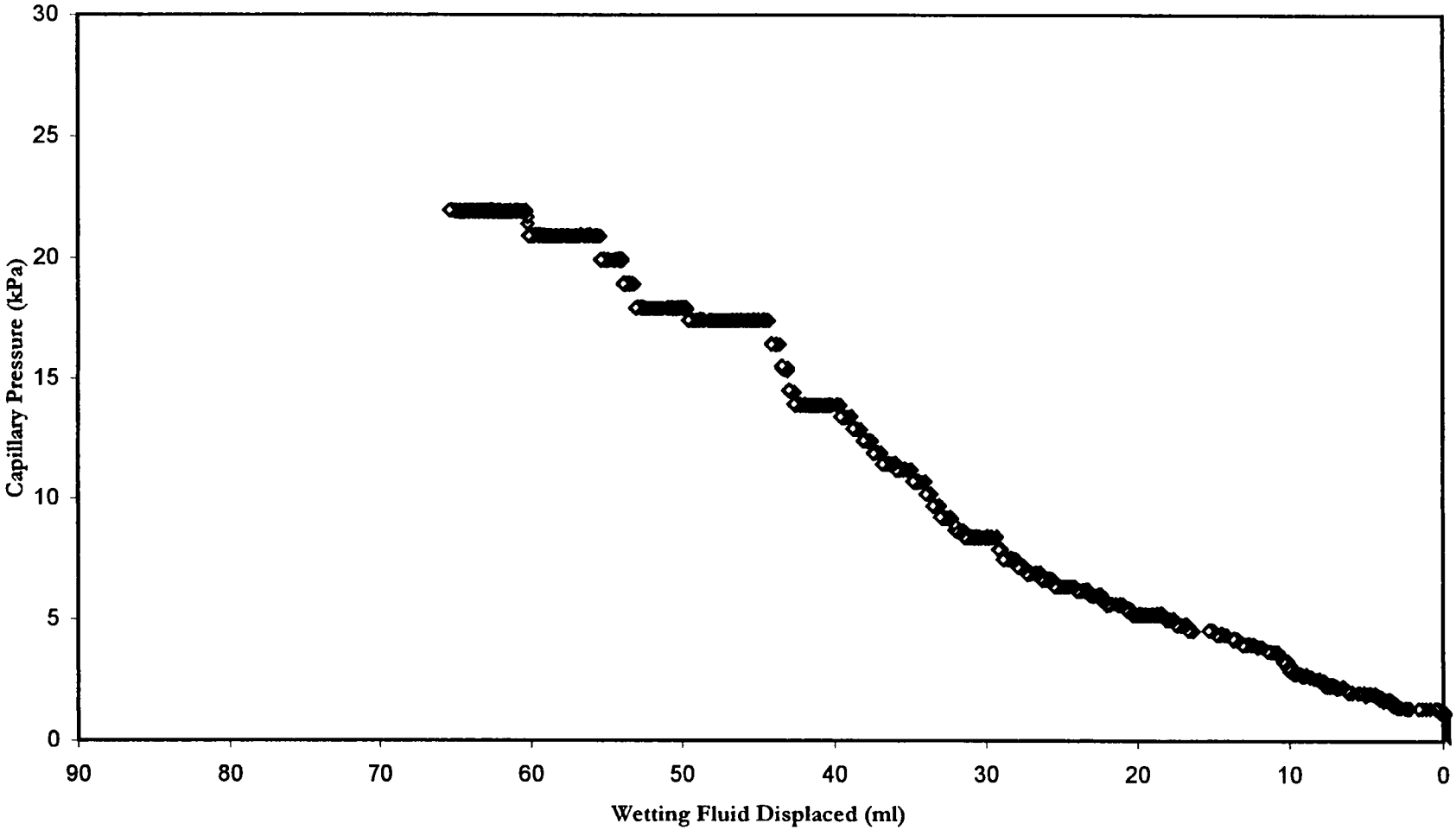

Figure 5. Results of Air-water injection.

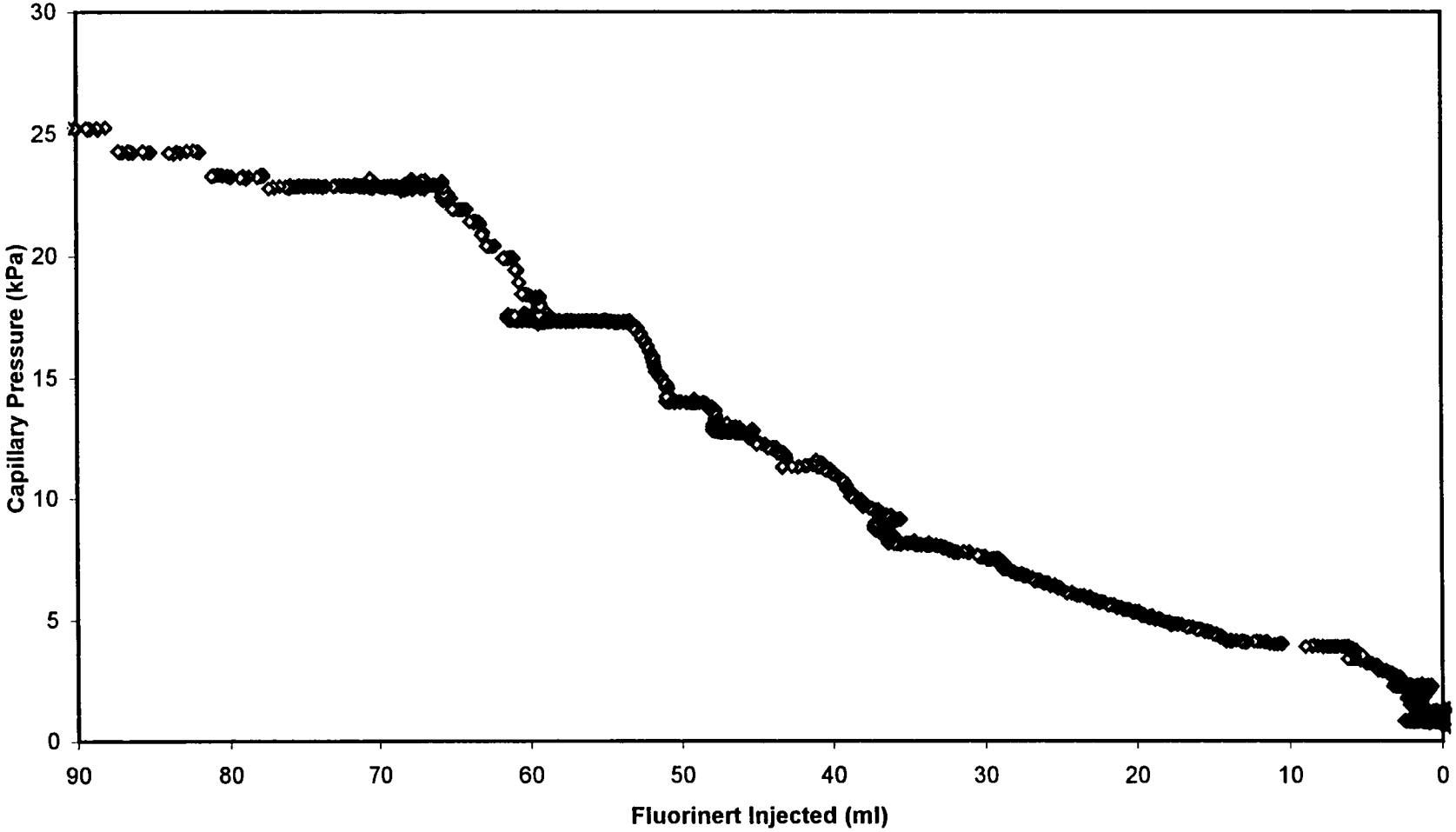

Figure 6. Results of Fluorinert-water injection.

and that the saturation fluid is perfectly wetting ($\theta = 0$), the fracture apertures corresponding to the measured air and Fluorinert initial entry pressures were calculated using equation 3. The results were 113 μm for the air and 142 μm for the Fluorinert. These values are significantly larger than the hydraulic aperture of 50 μm, and indicate that hydraulic apertures should not be used to predict the initial entry of a DNAPL into a fractured material. Because the hydraulic aperture is an "average" aperture calculated assuming that the fracture system is a uniform set of orthogonal, equally spaced, parallel plate fractures all of equal aperture, it is be expected that some fractures will be larger than this average aperture. Aperture values calculated from observed entry pressures are measures of the largest actual aperture open at the influent end of the sample.

Initial Matrix Entry

Prior to the injections, it was hypothesized, based on drainage behavior observed by Wilson et al. (1992), that fracture drainage would occur rapidly once the displacement fracture-entry pressure was exceeded, followed by a period of very little until the displacement entry pressure of the matrix was exceeded. It was expected that the initial matrix entry pressure could be identified as a significant displacement following multiple pressure increments with little or no displacement, much like the

behavior which identifies the initial fracture entry. As can be seen in Figures 5 and 6, the behavior or the curves are similar to each other, but the behavior is not as was hypothesized prior to the injections. Following the initial fracture entry, drainage continues in both cases in a more or less regular pattern until a pressure of roughly 17 kPa is attained. There is no cessation of drainage that would be a positive indication of the end of fracture drainage. There are at least two reasons which could explain the lack of a distinct indication of fracture drainage. If there is a significant percentage of matrix pores with much larger pore throats than most of the matrix, drainage from these pores would be hard to distinguish from fracture drainage. Alternatively, because there is a distribution of capillary pressures with height in the column, fracture drainage could still be occurring from parts of the sample when other parts of the fractures have ceased draining. The most likely explanation is some combination of these two effects.

Both curves change behavior beginning at a pressure of 17.09 kPa for the air and at 17.05 kPa for the Fluorinert where more significant drainage occurs for individual pressure increments. This change in behavior is interpreted to indicate that drainage from the matrix began. Assuming that the pores in the matrix are circular, and that the saturation fluid is perfectly wetting ($\theta = 0$), the pore radii calculated using equation 2 for initial entry into the matrix at these pressures was 8 μm for the air and 6 μm for the Fluorinert. These values are similar to the values reported by Dorsch and Katsube,

(1998) who indicated significant porosity in pores with radii larger than 5 μm. A direct comparison of initial entry values is not possible however, because they did not measure an initial entry pressure, or quantify porosity in pores larger than 5 μm.

The depth at which any DNAPL would enter pores of this size can be estimated given the density of the fluid and its interfacial tension. For example, if a water table existed at a depth of 0.5 meter below ground surface, and a continuous body of trichloroethene (density 1.487, interfacial tension 34.5 dynes/cm) extended from the ground surface, then the displacement entry pressure for pores with radius 6 μm (displacement entry pressure of 11.5 kPa from equation 2) would be invaded at a depth of only 1.4 meters. This result suggests that even a small DNAPL spill would result in migration of immiscible phase contaminants into the matrix pores of this material.

Fracture Volume

The total fracture volume determined from the air injection was 44.28 ml as compared to 52.94 ml determined from the Fluorinert. The difference between these values is most likely experimental error, because both fluids should theoretically occupy the same aperture sizes at the point of matrix entry. The fracture volumes correspond to porosity values of 0.026 and 0.031, which are six to eight times larger than the fracture porosity value of .004 predicted from the cubic law, but lower than

the range of .062 to .090 observed by Wilson et al. (1992) during laboratory drainage experiments. All of the calculated fracture porosity values are much smaller than the measured bulk porosity of 0.54, and other reported values which range from .35 to .47 (Wilson et al., 1992; Cumbie 1997). The drainage results are summarized in Table 2.

Air-Water Scaling

To evaluate the potential for estimating initial entry of DNAPL into fractures and into the clay matrix from air data, the predicted entry pressures for Fluorinert were calculated from the measured air data using equation 9, and compared to the observed Fluorinert entry pressures. The predicted value of fracture entry was 0.92 kPa, which was 126% of the observed entry pressure. The predicted matrix entry was 12.56 kPa, which was 74% of the observed pressure. The drainage behavior of Fluorinert as predicted from scaled values of the air drainage behavior is shown in Figure 7.

Contact angles were not measured for the fluid pairs used in the study. However, fracture entry overestimation and matrix entry underestimation suggests that differences in contact angle are not responsible for the lack of scaling agreement because a ratio of constant contact angles would produce either overestimation or

Table 2. Summary of air and Fluorinert injection results.

	Initial Fracture Entry	Calculated Aperture	Initial Matrix Entry	Calculated Pore Radius	Displaced Wetting Phase
Air	1.28 kPa	113 μm	17.39 kPa	8 μm	44.3 ml
Fluorinert	0.73 kPa	142 μm	17.05 kPa	6 μm	52.9 ml

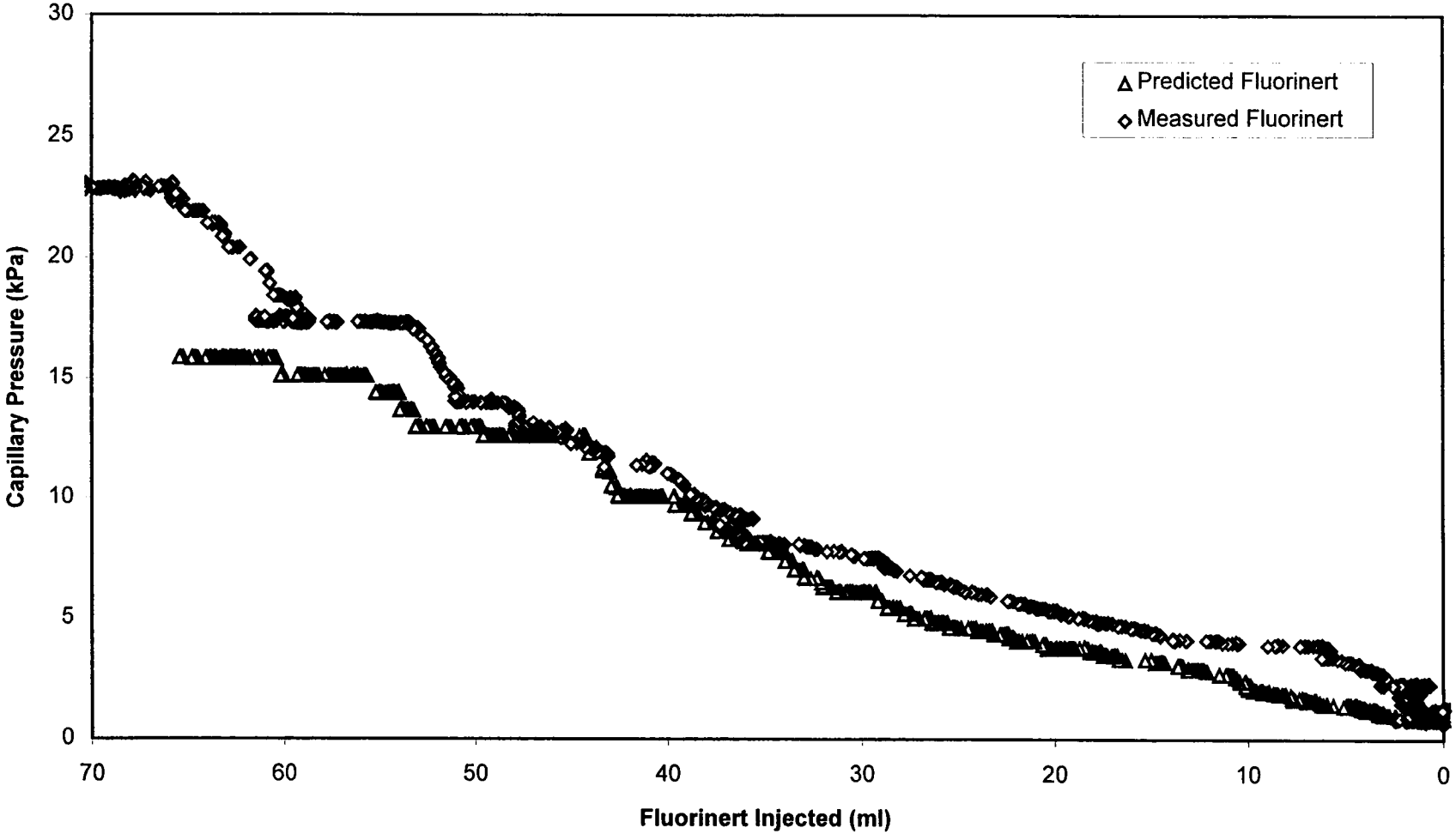

Figure 7. Comparison of predicted Fluorinert drainage curve to measured Fluorinert drainage curve.

underestimation in both cases. The similarity between the two drainage curves (Figures 5 and 6) suggests that air-water measurements could be used to estimate the general drainage behavior of a DNAPL in this material, and to estimate the fracture volume. The lack of agreement between the predicted and observed values for initial fracture and matrix entry suggests that air-water scaled predictions of DNAPL entry must be considered useful estimates, but not highly accurate representations of the behavior.

P_c-S Determination

Data produced during the injections consists of the pressure conditions at the sample influent (z_n) and effluent (z_w) levels and the saturation fluid (water) displaced or nonwetting fluid injected for given pressure conditions. For a traditional P_c-S relationship, the data need to be presented in the form of capillary pressure values as a function of saturation for the fracture system. Thus for each equilibrium condition, the displaced volume must be converted to a saturation, and the pressure conditions must be converted to a capillary pressure. Because the actual volume of the fractures is not known, the saturation of the fractures cannot be determined from the available data. However, the total volume of saturation fluid displaced during the fracture drainage can be considered the volume corresponding to irreducible saturation, because

at this point, the apertures from which drainage occurs are size equivalent to pores of the matrix porosity, and therefore are indistinguishable from matrix drainage. Based on this reasoning, the total fracture volume is assumed to be 105% of the total water displaced during fracture drainage, and saturations are calculated simply as a percentage of this volume. Using this reasoning and treating the matrix as impermeable, the measured drainage curves were overlain with conceptual curves showing the fracture drainage (Figure 8,9). These conceptual curves are intended to represent the fracture drainage independent of the matrix behavior.

If it is assumed that one capillary pressure is representative of the whole sample at each equilibrium condition as in the traditional approach, an elevation must be chosen as the most representative elevation of the sample, and capillary pressures would be calculated at the various pressure conditions at this elevation using equations 10 through 14. The capillary pressures shown in figures 5 through 9 were calculated at the sample influent level $z = z_c$. This elevation was chosen for these figures because the initial entry of immiscible phase into the fractures occurs at this elevation, thus the value calculated as the initial fracture entry pressure and the associated aperture calculated from this pressure are correct. Similarly, because in both injections the sample influent level is the elevation of greatest capillary pressure throughout the injection, this is also the elevation at which the first matrix entry occurred, and the

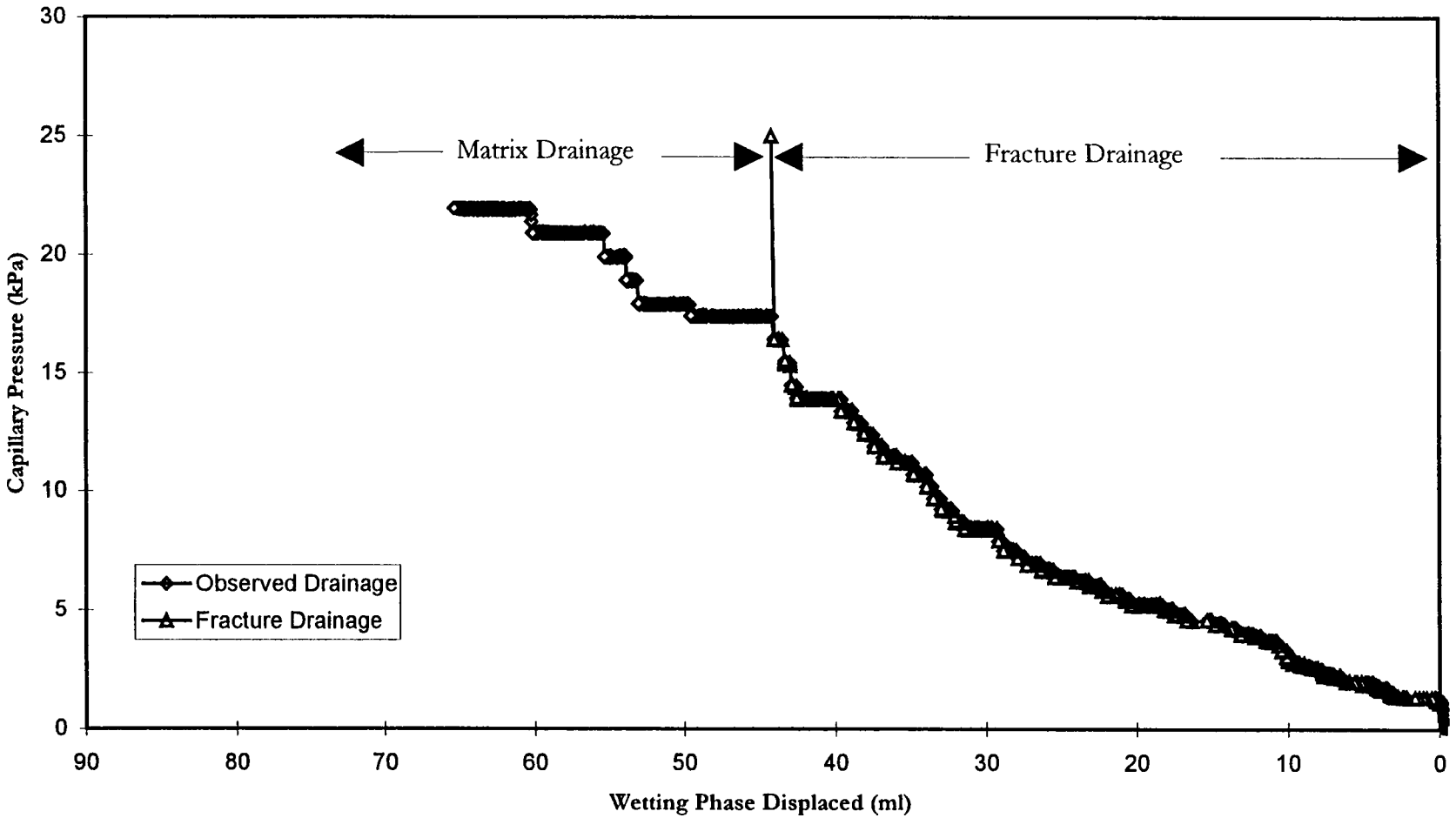

Figure 8. Air drainage conceptualized as separate fracture and matrix drainages.

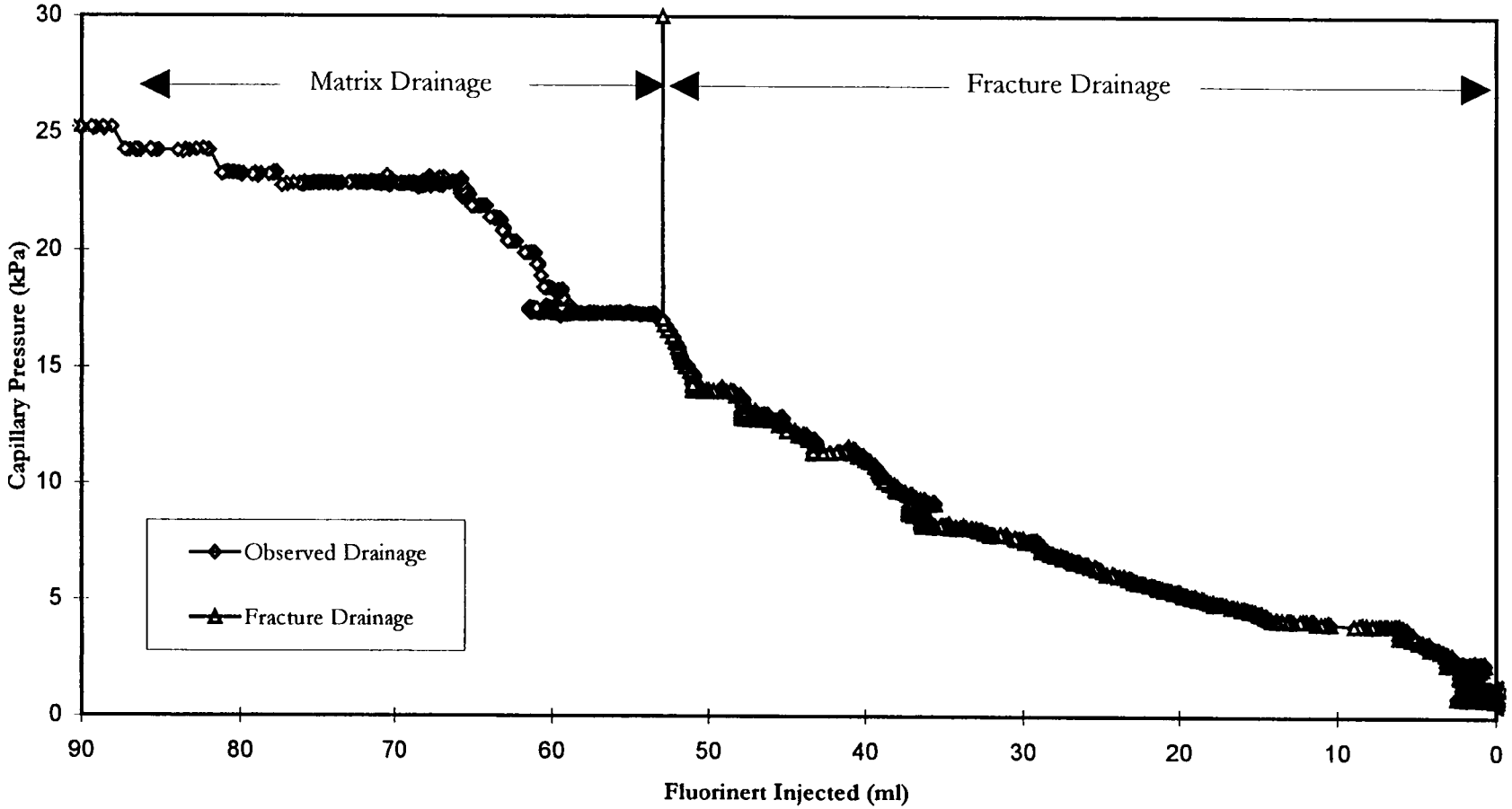

Figure 9. Fluorinert drainage conceptualized as separate fracture and matrix drainages.

initial entry pressure into the matrix and associated pore size calculated from it are also correct.

The effect of choosing other constant elevations within the sample to represent its capillary pressure is illustrated in figures 10 and 11. These figures were produced by plotting the capillary pressure calculated at three different constant elevations within the pressure cell using equations 10 through 14, and the average capillary pressure as a function of the wetting fluid saturation. The elevation curves represent the capillary pressure at the sample influent (z_n), sample effluent (z_w), and middle elevations. The average capillary pressure is simply the difference in the measured nonwetting ($\overline{P_n}$) and wetting ($\overline{P_w}$) fluid measurements measured at z_n and z_w respectively (Figure 2). As can be seen in Figures 10 and 11, when the elevation for calculation of the capillary pressure is moved from the influent end of the sample to the effluent end, the curve is shifted toward lower capillary pressures. Although the influent elevation was most representative for calculations of both the initial fracture entry pressure and the initial matrix entry pressure, as the interface between the two fluids moves away from this elevation during fracture drainage, this curve would become progressively less representative of the sample. Similarly, the effluent elevation would be the most accurate curve during final drainage of the fractures but least accurate for the early

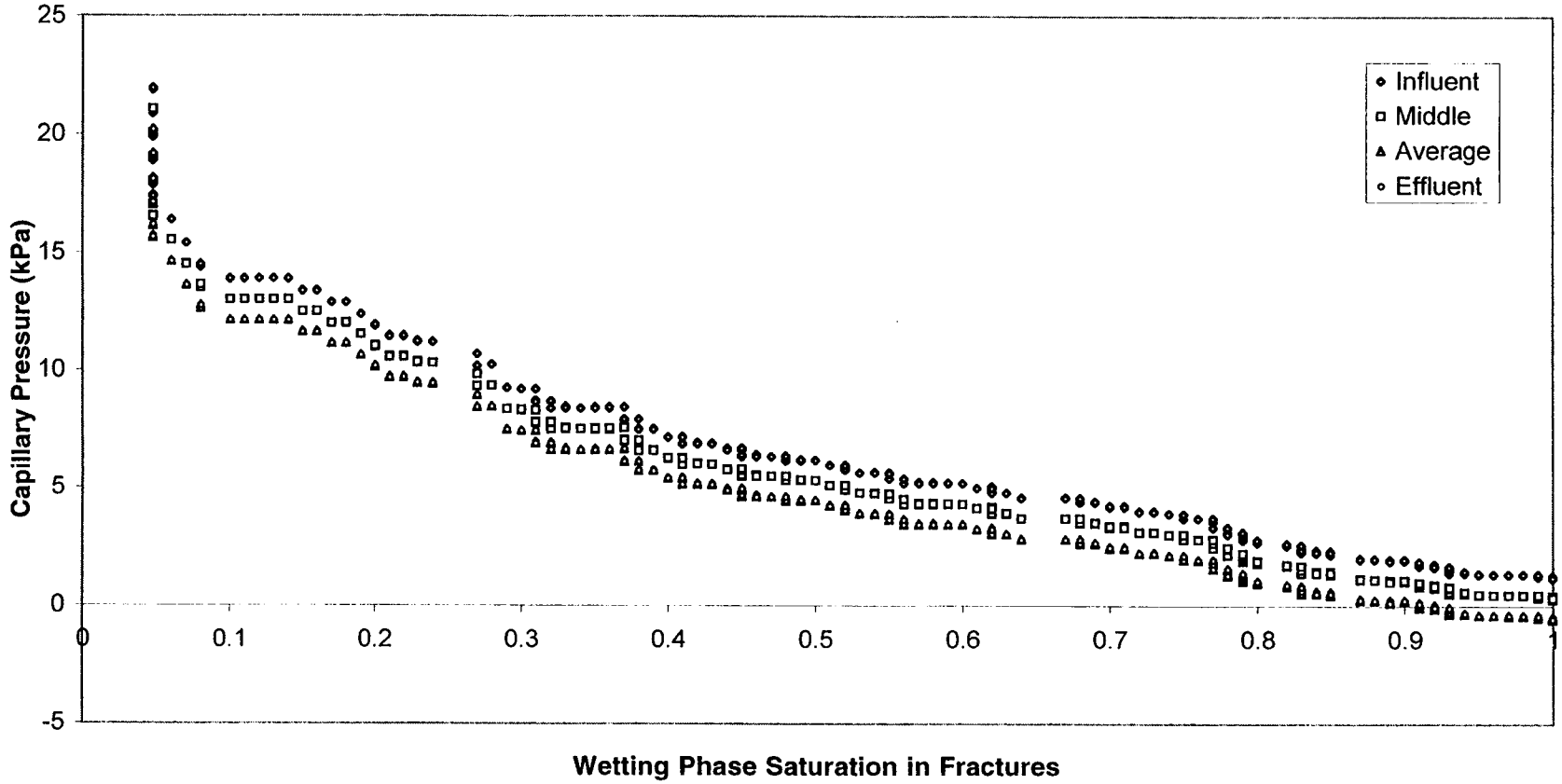

Figure 10. Plot showing the effect of choosing different constant elevations for calculation of capillary pressure on the air data. The influent and effluent curves were calculated using the influent and effluent elevations of the sample. The middle curve was calculated at the elevation of the midpoint of the sample. The average curve was calculated using the simple difference between the nonwetting and wetting phase pressures.

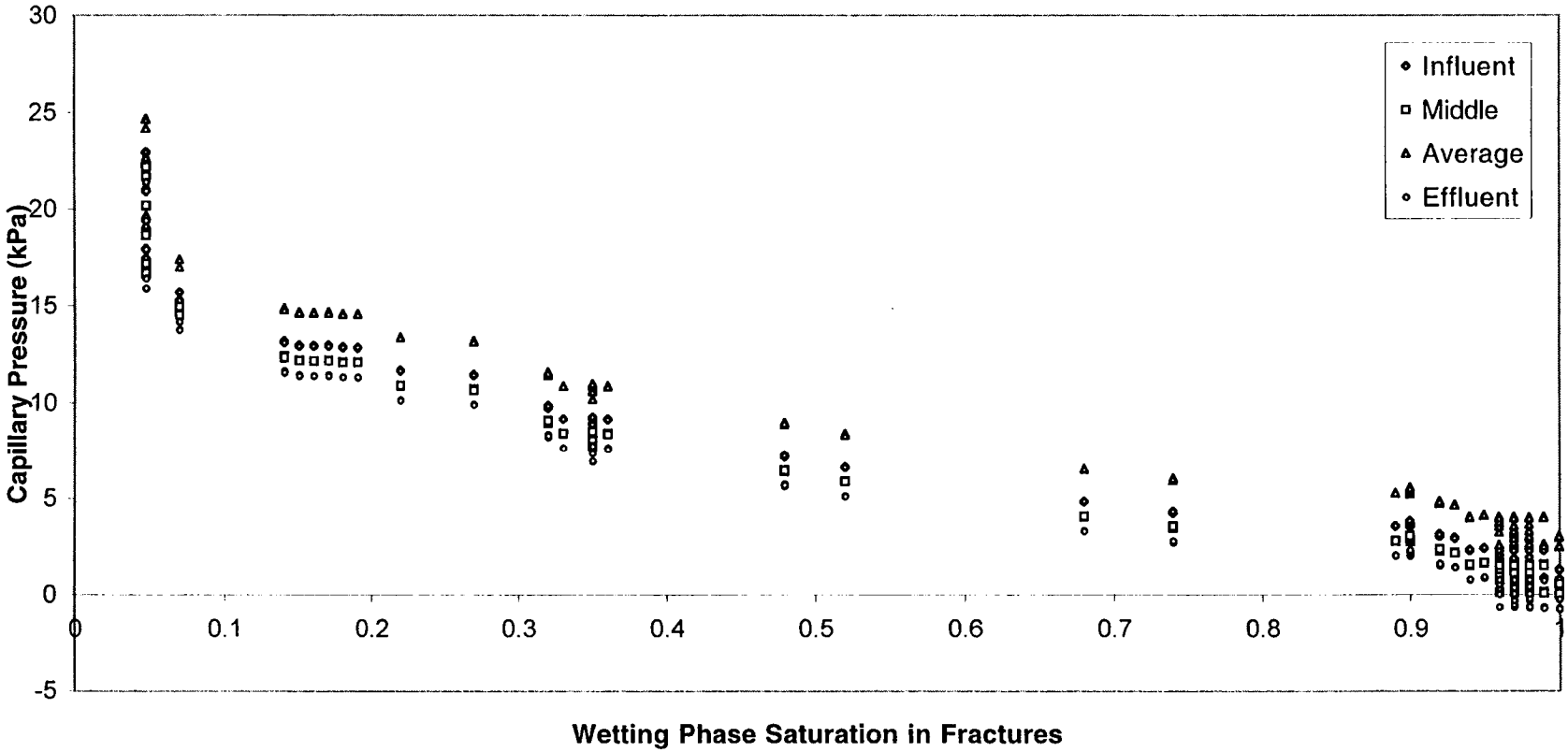

Figure 11. Plot showing the effect of choosing different constant elevations for calculation of capillary pressure on the Fluorinert data. The influent and effluent curves were calculated using the influent and effluent elevations of the sample. The middle curve was calculated at the elevation of the midpoint of the sample. The average curve was calculated using the simple difference between the nonwetting and wetting phase pressures.

drainage. These influent and effluent level curves represent the extremes of possible capillary pressures within the sample during drainage. In both cases, the effluent elevation curve inaccurately implies that drainage occurred before a positive capillary pressure was present in the sample.

Liu and Dane (1995) suggested that if the capillary pressure at one elevation is to be considered representative of a sample, then capillary pressures should be measured in the middle elevation of the sample. This suggestion was based on a sensitivity analysis done in unfractured porous materials. As can be seen in Figure 10, the middle elevation curve for the air data also inaccurately implies that drainage occurred before a capillary pressure was present. To be useful in fractured materials, a capillary pressure curve should accurately show the initial entry pressure, which is a critical parameter for predicting immiscible phase migration. Neither middle elevation curve does this. Because the average curves are not calculated at an elevation, they do not account for differences in fluid densities, and therefore produce different curves for different pressure-cell orientations for the same material. For the air orientation, the average curve duplicates the effluent curve. For the Fluorinert orientation, the average curve is shifted to higher capillary pressure, and incorrectly implies that no drainage occurs until capillary pressure is well above the initial fracture entry pressure. From this discussion it seems evident that no single elevation can represent the capillary pressure

of the whole sample well, but that the actual capillary pressure should lie between the influent and effluent curves.

Because the interface between immiscible fluids is assumed to move through the sample during the drainage, the elevation used to calculate the capillary pressure should move through the sample with the interface. This assumption is not applicable in reality because the interface is not a plane moving through the sample. For given pressure conditions, the interface would be at different elevations within fractures of different apertures. Liu and Dane (1995) derived a relation to predict the elevation of the boundary between saturated and unsaturated zones of the wetting fluid in an unfractured homogeneous material. Adapted to the given application, the elevation is given by

$$z_{cr} = \frac{P_d - \overline{P_n} + \overline{P_w} - g(\rho_n z_n + \rho_w z_w)}{g(\rho_w - \rho_n)} \qquad \text{when } \rho_n < \rho_w \qquad (16)$$

$$z_{cr} = \frac{P_d - \overline{P_n} + \overline{P_w} - g(\rho_w z_w - \rho_n z_n)}{g(\rho_n - \rho_w)} \qquad \text{when } \rho_n > \rho_w \qquad (17)$$

where z_{cr} is the calculated elevation of the interface, P_d is the initial entry pressure, g is the acceleration due to gravity, ρ_n and ρ_w are the densities of the nonwetting and wetting fluids respectively, and $\overline{P_n}, \overline{P_w}, z_n, z_w$ are all as defined in figures 2 and 4.

Because this relation will calculate elevations < 0 and $> z_c$, which have no meaning, Liu and Dane (1995) defined an alternative variable z^* to describe the interface given by

$$z^* = 0 \qquad \text{for } z_{cr} \leq 0 \tag{18}$$

$$z^* = \min[z_c, z_{cr}] \quad \text{for } z_{cr} > 0 \tag{19}$$

When this relation is applied to the measured data during fracture drainage, the result is a calculated interface that begins at the influent elevation at initial entry into the fractures, moves quickly to the effluent level with increased pressure, and then stays at this level through most of the drainage. This relation was intended by the authors to identify the elevation of the interface between complete and partial saturation of the wetting fluid in granular materials, based on the pressure conditions and initial entry pressure of the sample. If it is applied to fractured materials, it represents the location of the interface in the largest fracture present, and assumes that this fracture has constant aperture throughout the length of the sample. Figures 12 and 13 show the capillary pressure curve resulting when the moving interface defined by equations 16 and 19 is applied to equations 10 through 14. The influent and effluent level curves from figures 10 and 11 are also plotted for comparison. As can be seen, the Liu and Dane (1995) moving interface curves well represent the initial entry pressures in both cases, remain constant at the initial fracture entry pressure as the interface

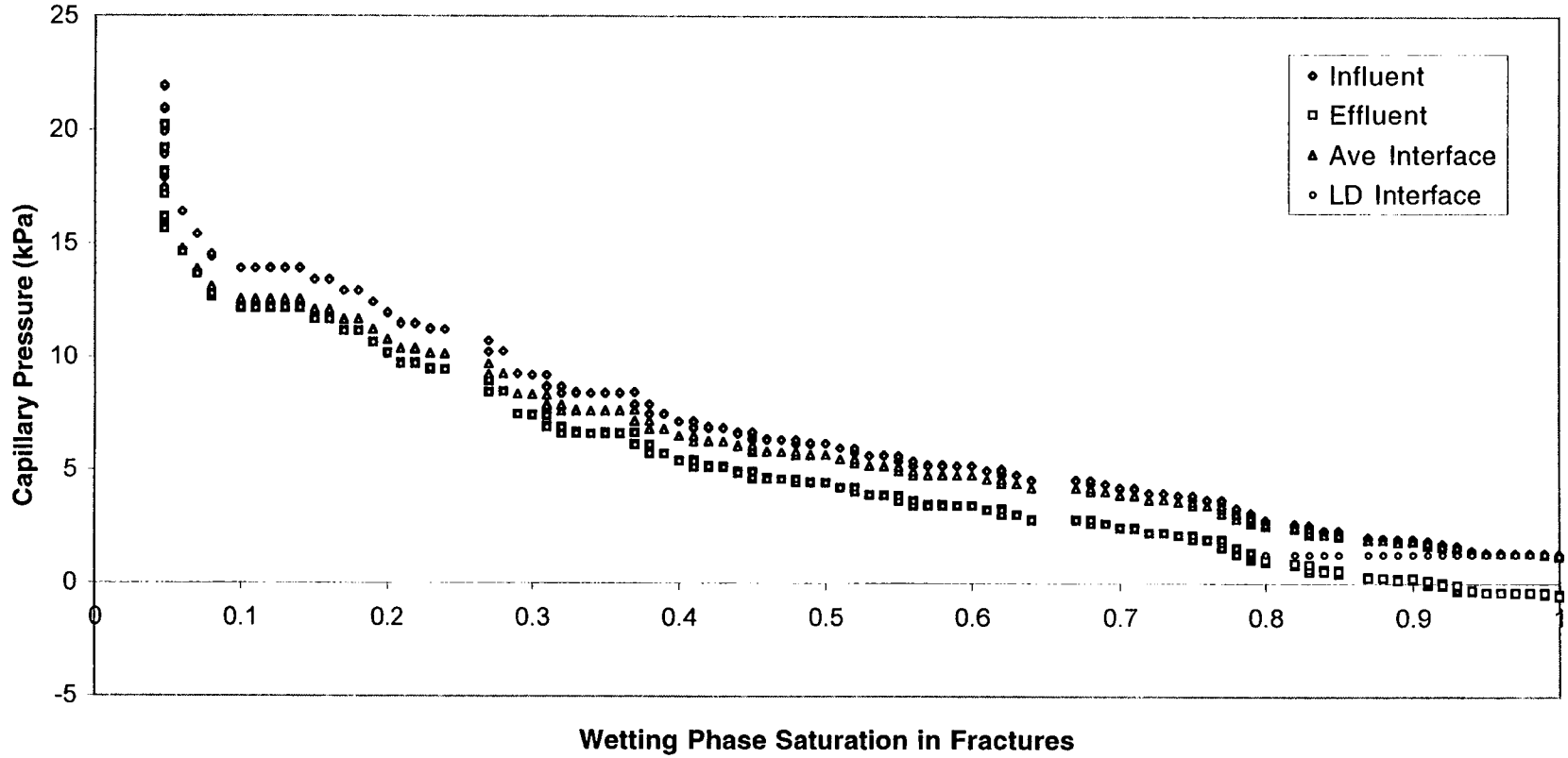

Figure 12. Plot showing capillary pressure calculated for the air data using the Liu and Dane (1995) moving interface (LD Interface), and the "average" interface (Ave Interface). The constant influent and effluent curves from Figure 10 are also plotted for comparison.

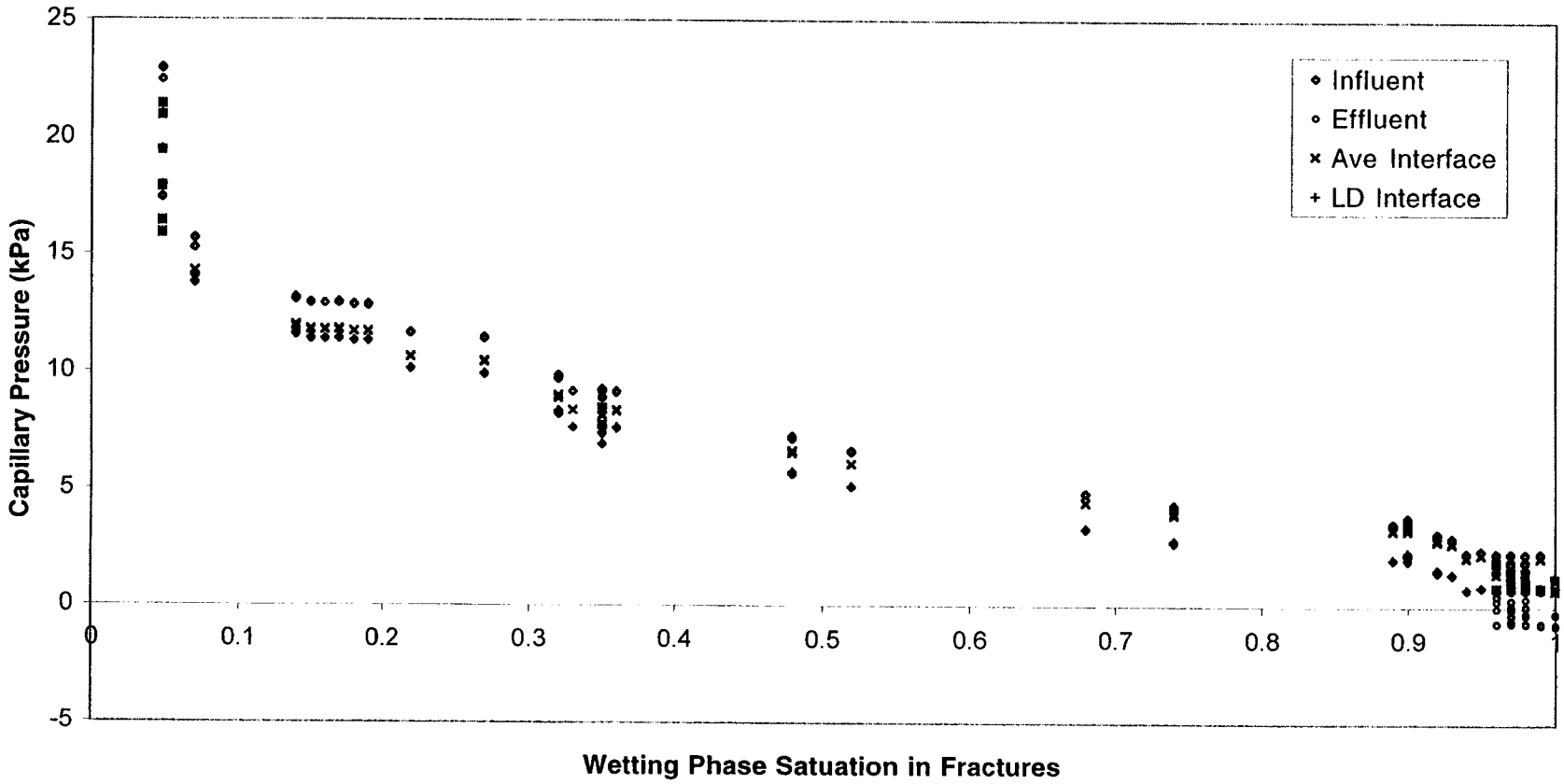

Figure 13. Plot showing capillary pressure calculated for the Fluorinert data using the Liu and Dane (1995) moving interface (LD Interface), and the "average" interface (Ave Interface). The constant influent and effluent curves from

moves through the sample, and then duplicate the effluent level curves. These curves can be expected to represent the capillary pressure over the whole drainage curve better than either the influent or effluent curves because both of those curves are very inaccurate at one extreme or the other. The Liu and Dane moving interface may not be the best representation of the location of the interface however, because it is based on only the largest fracture in the sample. Thus z^* goes to z_w when the immiscible phase has moved the length of the sample within the largest fracture of the sample.

A better representation of the moving interface may be one that defines it as moving with the immiscible phase in the average sized fracture in the sample. There are only two points during the drainage when the location of the interface is known or can be inferred and can be represented by a plane. The location of the interface is known to be at the influent elevation (z_n) at capillary pressures between 0 and the initial entry pressure, and can thus be represented by a plane. If it is assumed that fracture drainage has just reached irreducible saturation when the matrix drainage begins, which is valid when pores of the matrix are much smaller than the fracture apertures, it follows that the interface has reached the effluent level (z_w) in all fractures, and again can be represented by a plane. Although it is expected that the location of the interface is very erratic and not well represented by a plane at any point between influent and effluent levels, an approximation can be made for the location of the

interface if it is assumed that the interface is a plane that moves linearly between the influent and effluent levels. This elevation z_a is given by

$$z_a = z_c - \left[\frac{z_c (P_i - P_f)}{(P_m - P_f)} \right] \tag{20}$$

where z_a is the elevation of the "average" interface, z_c is the sample length, P_i is the capillary pressure calculated at the soil influent level, P_f if the initial entry pressure into the fractures, and P_m is initial entry pressure into the matrix. As in the case of the Liu and Dane relation, this relation will produce values for $z_a < 0$ and $> z_c$, which have no meaning, so another variable must be defined by

$$z_i = 0 \qquad \text{for } z_a \leq 0 \tag{21}$$

$$z_i = \min[z_c, z_a] \qquad \text{for } z_a > 0 \tag{22}$$

where z_i is the elevation of the "average" interface. The result of using this relation to estimate the interface is a moving interface that progresses evenly from influent end to effluent end as a function of the capillary pressure. This approximation of the interface would be most accurate when the fracture network is uniform from top to bottom. The drainage curves in the present study indicate that this might be true for the saprolite sample, because the rate of drainage with pressure increase did not drastically change during either injection, and the data do not indicate that fractures drained

completely before matrix drainage began. Figures 12 and 13 show the P_c-S curves resulting from using equations 20 through 22 to calculate the location of the interface at given pressure conditions, and then using this elevation in equations 10 through 14. This curve is accurate at the initial entry pressure, then steadily approaches the effluent elevation curve at the residual saturation. Although an approximation, these curves should represent the capillary pressure of a tall column better than any constant elevation.

Brooks and Corey Curve Fits

A nonlinear least-squares optimization code (van Genuchten et al., 1991) was used to fit the average interface P_c-S air and Fluorinert curves to both the Brooks and Corey (1964) and van Genuchten (1980) models (Figure 14, 15, Table 3, 4). The 95% confidence intervals for these fits are shown in Table 5. As shown in Figures 14 and 15, the Brooks and Corey fits (BC Fit) were poor at both extremes of saturation when all fitting parameters were optimized by the code. The initial entry pressure produced by this fit was much above the observed value (Tables 3 and 4). When the initial entry pressure parameters were fixed at the observed values and the other parameters were optimized by the code, the fits (BC Fixed Entry) were worse, as can be seen visually in

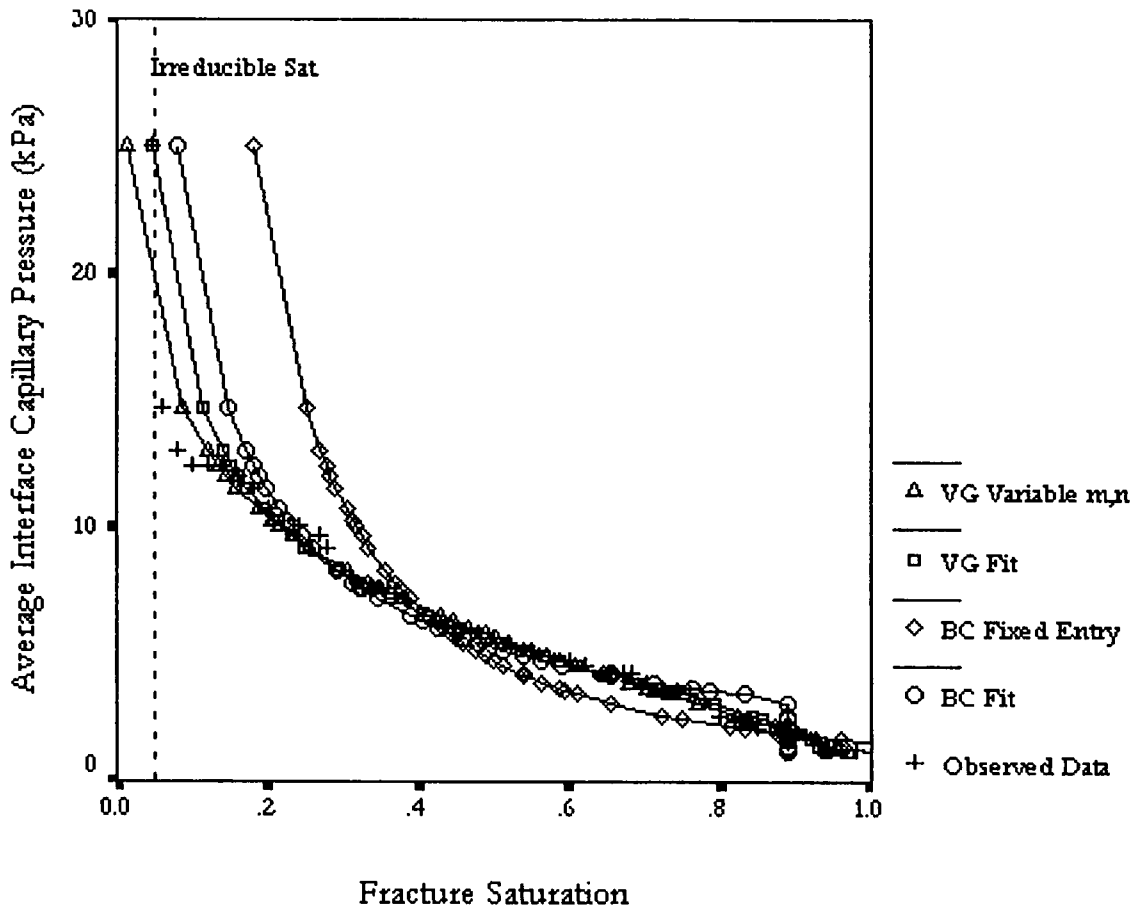

Figure 14. Brooks and Corey (BC Fit and BC Fixed Entry) and van Genuchten (VG Fit and VG Variable m,n) fits to the "average" interface calculated for the air injection data. The BC Fit line was fit allowing all parameters to be optimized. The BC Fixed Entry line was fit by fixing the initial fracture entry pressure at the observed value, and the other parameters were optimized. The VG Fit optimized all parameters using the assumption of Mualem (1976). The VG Variable m,n fit assumed no fixed relation between the m and n parameters.

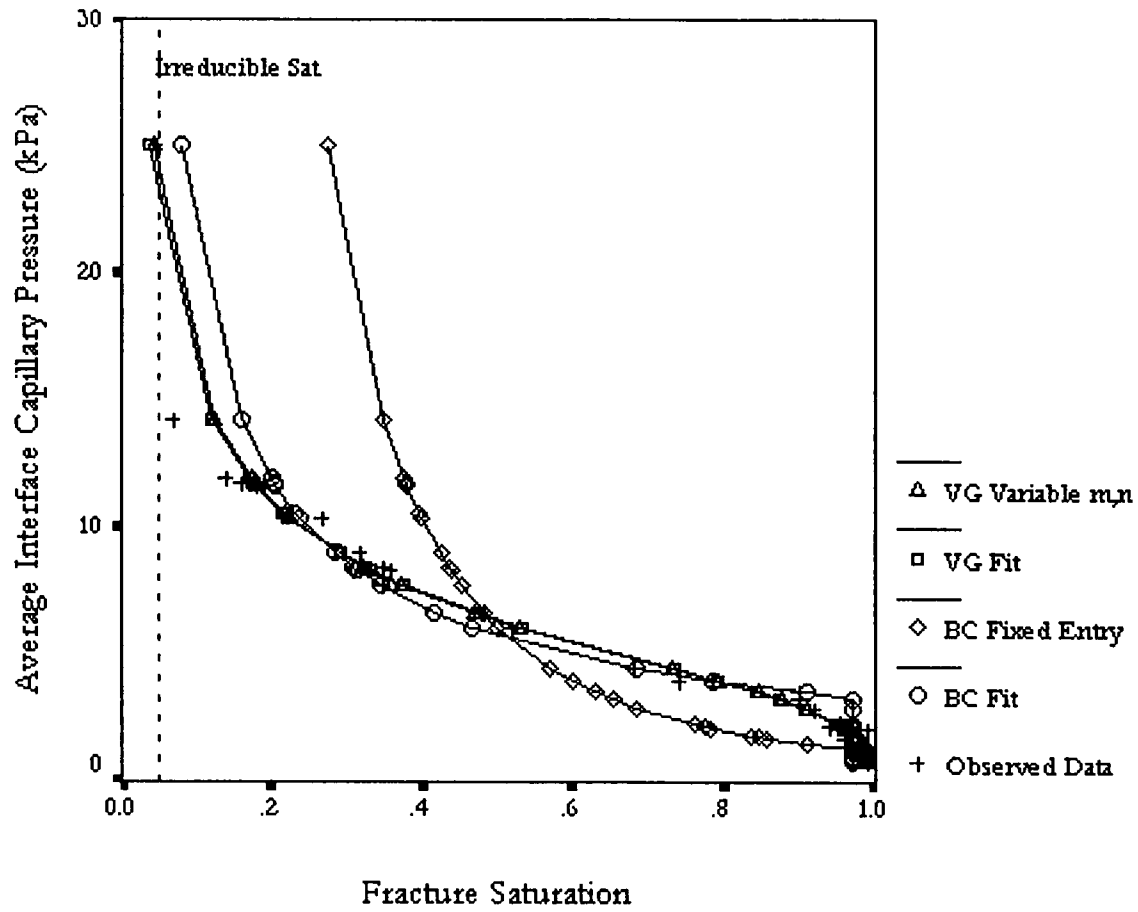

Figure 15. Brooks and Corey (BC Fit and BC Fixed Entry) and van Genuchten (VG Fit and VG Variable m,n) fits to the "average" interface calculated for the Fluorinert injection data. The BC Fit line was fit allowing all parameters to be optimized. The BC Fixed Entry line was fit by fixing the initial fracture entry pressure at the observed value, and the other parameters were optimized. The VG Fit optimized all parameters using the assumption of Mualem (1976). The VG Variable m,n fit assumed no fixed relation between the m and n parameters.

Table 3. Best fit Brooks and Corey and van Genuchten parameters to air injection data. Brooks and Corey parameters are S (initial saturation), S_r (residual saturation), λ (fitting parameter), and P_f (initial fracture entry pressure). The van Genuchten parameters are S (initial saturation), S_r (residual saturation), α, m, and n (fitting parameters). SSQ is the residual sum of squares, which is minimized by the RETC code.

	S	S_r	λ	P_f	α	m	n	SSQ
BC Fit	0.8892	0	1.1802	3.24 kPa				0.1110
BC Fixed Entry	1.1230	0	0.6129	1.28 kPa				0.4870
VG Fit	0.9543	0			0.2194	0.6403	2.7804	0.0316
VG Variable m ,n	1.0370	0			0.0753	3.1532	1.5861	0.0216

Table 4. Best fit Brooks and Corey and van Genuchten parameters to Fluorinert injection data. Brooks and Corey parameters are S (initial saturation), S_r (residual saturation), λ (fitting parameter), and P_f (initial fracture entry pressure). The van Genuchten parameters are S (initial saturation), S_r (residual saturation), α, m, and n (all fitting parameters). SSQ is the residual sum of squares, which is minimized by the RETC code.

	S	S_r	λ	P_f	α	m	n	SSQ
BC Fit	0.9691	0	1.2378	3.35 kPa				0.0455
BC Fixed Entry	1.2195	0	0.4207	0.73 kPa				1.2172
VG Fit	0.9946	0			0.1876	0.6790	3.1153	0.0231
VG Variable m ,n	0.9914	0			0.2023	0.5734	3.3748	0.0228

Table 5. The 95% confidence intervals for parameters corresponding to best fits shown in figures 14 and 15.

S		Air			Fluorinert	
	Best	Upper	Lower	Best	Upper	Lower
BC Fit	0.8892	0.9177	0.8606	0.9691	0.9835	0.9547
BC Fixed Entry	1.1230	1.2083	1.0376	1.2195	1.3497	1.0894
VG Fit	0.9543	0.9769	0.9316	0.9946	1.0078	0.9814
VG Variable	1.0370	1.0960	0.9779	0.9914	1.0072	0.9756
λ		Air			Fluorinert	
	Best	Upper	Lower	Best	Upper	Lower
BC Fit	1.1802	1.2942	1.0672	1.2378	1.3317	1.1439
BC Fixed Entry	0.6129	0.6880	0.5378	0.4207	0.5138	0.3277
P_f		Air			Fluorinert	
	Best	Upper	Lower	Best	Upper	Lower
BC Fit	3.24	3.44	3.07	3.35	3.5161	3.1949
BC Fixed Entry	1.28	1.28	1.28	0.73	0.73	0.73
α		Air			Fluorinert	
	Best	Upper	Lower	Best	Upper	Lower
VG Fit	0.2194	0.2307	0.2081	0.1876	0.1964	0.1788
VG Variable	0.0753	0.1631	-0.0125	0.2023	0.2405	0.1641
m		Air			Fluorinert	
	Best	Upper	Lower	Best	Upper	Lower
VG Fit	0.6403	0.6570	0.6219	0.6790	0.6956	0.6605
VG Variable	3.1532	7.5030	-1.1967	0.5734	0.8258	0.3210
n		Air			Fluorinert	
	Best	Upper	Lower	Best	Upper	Lower
VG Fit	2.7804	2.9158	2.6450	3.1153	3.2853	2.9452
VG Variable	1.5861	2.0071	1.1651	3.3748	4.1567	2.5928

Figures 14 and 15 and indicated by larger residual sum of squares (SSQ) in Tables 3 and 4. The van Genuchten (1980) model was used to fit the data (VG Fit) following the predictive model of Mualem (1976) for unsaturated flow and allowing all parameters to be optimized. The Mualem (1976) model is given by

$$n = (1 - m)^{-1} \tag{23}$$

The van Genuchten model was also used to fit the data with n and m parameters independent of each other (VG Variable m,n) the most general form of the van Genuchten (1980) relation. As can be seen in Figures 14 and 15, and supported by smaller residual sum of squares in Tables 3 and 4, the van Genuchten model produced better fits to the observed data than the Brooks and Corey (1964) model. The best fits were obtained with the most general form (VG Variable m,n), but the fit was poor at the extremes of saturation.

CONCLUSIONS AND IMPLICATIONS

This study has shown that air-water measurements of drainage behavior in a tall sample of fractured shale saprolite can be a useful tool for the characterization of DNAPL behavior in this, and likely in other fractured clay-rich materials. The air-water measurements provided estimates of the initial fracture entry pressure, initial matrix entry pressure, and fracture volume, all of which are needed to model the behavior and distribution of DNAPLs in fractured materials. The initial fracture entry pressure and fracture volume determined by this method are significantly larger than cubic-law-derived approximations of these parameters. Although scaling of air-water measurements to predict Fluorinert initial entry pressures into the fractures and matrix was not exact (± 26%), scaled estimates are useful as first approximations when DNAPLs cannot be measured directly. The lack of agreement between observed and scaled estimates are expected to be small relative to the natural variability of fracture aperture and matrix pore sizes in this material. Further study is needed to determine the spatial variability of initial entry pressures in this material.

This study has also shown that the distribution of pressures within a soil column due to differences in immiscible fluid densities should be considered when capillary pressures are determined for a tall sample of material. When the initial entry pressures

are being determined, capillary pressure should be calculated at the sample influent level, because this is the elevation where initial fracture and matrix entry will likely occur. If a single, constant elevation must be used for calculation of the capillary pressure throughout the drainage of a tall sample, the mid-point elevation of the sample should be used. However, the accuracy of this representation will decrease as sample height increases, and it may misrepresent the critical initial entry pressures into both the fractures and the matrix.

Although the interface between immiscible fluids in a fractured material is expected to be highly erratic, and its elevation cannot be determined in a traditional pressure-cell setup, a method to approximate the "average" location of the interface as it moves through the sample during drainage has been proposed. The approximation should represent the capillary pressure within a tall sample better than any single constant elevation. The Brooks and Corey (1964) model failed to represent the "average interface" Pc-S behavior determined for the air-water and Fluorinert-water drainages during this investigation. This result contrasts with a previous study (Reitsma and Kueper, 1994) where the Brooks and Corey (1964) model provided a good description of immiscible fluid behavior in a single fracture in limestone. The van Genuchten model (1980) representation was better in the current study, but it is not yet clear if existing porous media functions are directly applicable to complex fracture systems, such as occur in the saprolite.

The study suggests that air-water Pc-S data that already exist for many materials, or that can easily be determined, can be used to estimate DNAPL-water behavior. The low fracture and matrix entry pressures for Fluorinert suggest that hazardous DNAPLs such as trichloroethene and perchloroethene will easily enter the fractures of this material, and may enter the matrix at relatively small "ponding" heights of a few meters or less. Entry into the matrix will tend to decrease the volume of saprolite contaminated by a spill of a given volume, but may also make it more difficult to remove the DNAPL because much of it will be in the small matrix pores.

LITERATURE CITED

LITERATURE CITED

3M, Fluorinert™ Liquids, Electronic Products Division, Austin, Texas, 1995.

Brooks, R. H., and A. T. Corey, Hydraulic properties of a porous media, Hydrology Paper no. 3, Colorado State University, Fort Collins, CO, 1964.

Corey, A. T., Mechanics of Immiscible Fluids in Porous Media, Water Resources Publications, Littleton, Colo., 1986.

Cumbie, D. H., Laboratory scale investigations into the influence of particle diameter colloid transport in highly weathered and fractured shale saprolite, MS Thesis, Dept. of Geological Sciences, Univ. of Tenn., Knoxville, 1997.

Dorsch, J. O., and T. J. Katsube, Petrophysical characteristics of saprolite from the Maryville Limestone/Dismal Gap Formation at Solid Waste Storage Area (SWASA) 7 on the Oak Ridge Reservation, Unpublished Report, 1998.

Dreier, R. B., D. K. Soloman, and C. M. Beaudoin, Fracture characterization in the unsaturated zone of shallow land burial facility, flow and transport through unsaturated fractured rock; eds. D. D. Evans and T. J. Nicholson, Geophysical Monograph, vol 42, pp. 51-59, 1987.

Dumore, J. M., and R. S. Scholls, Drainage capillary pressure functions and the influence of connate water, Soc. Pet. Eng. J., 14:437-444, 1974.

Harton, A., Influence of flow rate on transport of bacteriophage in a column of highly weathered and fractured shale, MS thesis, Dept. of Geological Sciences, University of Tennessee, Knoxville, 1996.

Hatcher, R. D., Jr., P. J. Lemiszki, R. B. Drier, R. H. Ketelle, R. R.. Lee, D. A. Leitzke, W. M. McMaster, J. L. Foreman, and S. Y. Lee, Status report on the geology of the Oak Ridge Reservation, Oak Ridge National Lab, ORNL/TM-12074, 1992.

Haun, D. B., L.D. McKay, and J. F. McCarthy, The role of electrostatic attachment on particle transport in fractured shale saprolite, Abstract presented at Conference on Mass Transport in Fractured Aquifers and Aquitards, Univ. of Copenhagen, Denmark, May 14-16, 1998.

Jardine, P. M., G. V. Wilson, and R. J. Luxmoore, Modeling the transport of inorganic ions through undisturbed soil columns from two contrasting watersheds, Soil Sci. Soc. Am. J., 52:1252-1259, 1988.

Jardine, P. M., G. K. Jacobs, and G. V. Wilson, Unsaturated transport processes in undisturbed heterogeneous porous media: I. Inorganic Contaminants, Soil Sci. Soc. Am. J., 57:945-953, 1993.

Klute, A., Water Retention: Laboratory Methods, In Methods of Soil Analysis, Part 1, Second Edition, ed. A. Klute, Am. Soc. Agron., Madison, Wisconsin, 1986.

Kueper, B. H., W. Abbot, and G. Farquhar, Experimental observations of multiphase flow in heterogeneous media, J. Contam. Hydrol., 5:83-95, 1989.

Kueper, B. H., D. B. McWhorter, The behavior of dense, nonaqueous phase liquids in fractured clay and rock, J. Groundwater, 29(5), 716-728, 1991.

Lenhard, R. J., and J. C. Parker, Measurement and prediction of saturation-pressure relationships in three-phase porous media systems, J. Contam. Hydrol., 1:407-424, 1987.

Lin, C., George F. Pinder, and E. F. Wood, Water Resources Program Report 83-WR-2, Water Resources Program, Princeton, N. J., Princeton University, 1982.

Liu, H. H., and J. H. Dane, Improved computational procedure for retention relations of immiscible fluids using pressure cells, Soil Sci. Soc. Am. J., 59:1520-1524, 1995.

Mualem, Y., A new model for predicting the hydraulic conductivity of unsaturated porous media, Water Resour. Res., 12(3), 513-522, 1976.

O'Brien, R. O., P. M. Jardine, J. P. Gwo, L. D. McKay, and A. D. Harton, Experimental and numerical evaluation of solute transport processes in fractured saprolites, Unpublished Report, 1996.

Penfield, C., Petrographic, mineralogical, and chemical characterization of soil and saprolite at the SWSA-7 Site Oak Ridge National Laboratory, Tennessee, Unpublished Report, 1998.

Reedy, O. C., P. M. Jardine, G. V. Wilson, and H. M. Selim, Quantifying the diffusive mass transfer of nonreactive solutes in columns of fractured saprolite using flow interruption. Soc. Soil Sci. Am. J., 60: 1376-1384, 1996.

Reitsma, S., and B. H. Kueper, Laboratory measurement of capillary pressure-saturation relationships in a rock fracture, Water Resour. Res., 30(4):865-878, 1994.

Rothschild, E. R., D. D. Huff, C. S. Haase, R. B. Clapp, B. P. Spalding, C. D. Farmer, and N. D. Farrow, Geohydrologic characterization of proposed waste storage area (SWSA) 7, Oak Ridge National Lab, ORNL/TM-9314, 1984.

Su, C., and R. H. Brooks, Soil hydraulic properties from drainage test, in Watershed Drainage Proceedings, pp. 516-542, American Society of Civil Engineers, New York, 1975.

Slough, K. J., E. A. Sudicky, and P. A. Forsyth, Importance of rock matrix entry pressure on DNAPL migration in fractured geologic materials, Ground Water, in-review (accepted pending minor revisions).

Snow, D. T., Rock fracture spacings, openings, and porosities, J. Soil Mech. Found. Div. Am. Soc. Civ. Eng., 94(SM1), 73-91, 1968.

Snow, D. T., Anisotropic permeability of fractured media, Water Resour. Res., 5(6):1273-1289, 1969.

van Genuchten, M. Th., A closed-form equation for predicting the hydraulic conductivity of unsaturated soils, Soil Sci. Soc. Am. J., 44:892-898, 1980.

van Genuchten, M. Th, F. J. Leij, and S. R. Yates, The RETC code for quantifying the hydraulic functions of unsaturated soils, U. S. Salinity Laboratory, USDA, EPA/600/2-91/065, 1991

Wilson, G. V., J. M. Alfonsi, and P. M. Jardine, Spatial variability of saturated hydraulic conductivity of the subsoil of two forested watersheds, Soil Sci. Soc. Am. J., 53:679-685, 1989.

Wilson, G. V., P. M. Jardine, and J. P. Gwo, Modeling the hydraulic properties of a multiregion soil, Soil Sci. Soc. Am. J., 56:1731-1737, 1992.

Wilson, G. V., P. M. Jardine, J. D. O'Dell, and M. Collineau, Field-scale transport from a buried line source in variably saturated soil, J. Hyrol., 145:83-109, 1993.

VITA

Samuel Clark Cropper was born in Gamaliel, Kentucky on July 28, 1963. He is the son of Jack L. Cropper and Drucilla A. Lee. He attended public school in Gamaliel, Kentucky and graduated in 1981. After attending Tennessee Technological University briefly and working various jobs, he married Cheri J. England in 1985 and moved to Tennessee. A physical geology correspondence course sparked an interest in earth science, and he entered Middle Tennessee State University in 1991, where he also developed an interest in computer science. He graduated *Magna Cum Laude* in May, 1995 with a Bachelor of Science degree in geology and a minor in computer science. He entered the Master's program in Geology at The University of Tennessee, Knoxville in June, 1995 and focused his studies on contaminant hydrogeology. He officially received the Master's degree in December, 1998. In August, 1998 he began his career as a geologist with Exxon Exploration Company in Houston, Texas.